

LASER BEAM WELDING OF ALUMINIUM ALLOYS

*A thesis submitted towards partial fulfillment of the requirements
for the degree of*

Master of Technology in Laser Technology

Course affiliated to Faculty of Engineering and Technology and
offered by Faculty Council of Interdisciplinary Studies, Law and Management,
Jadavpur University

submitted by

SOURADIP PAUL

Examination Roll No. : M4LST19008

Registration No. : 141049 of 2017-2018

Under the guidance of

DR. SOUREN MITRA

Professor, Production Engineering Department
Jadavpur University, Kolkata - 700032

School of Laser Science and Engineering

Faculty Council of Interdisciplinary Studies, Law and Management

Jadavpur University

Kolkata -700032

India

2019

M.TECH IN LASER SCIENCE AND TECHNOLOGY

Course affiliated to

FACULTY OF ENGINEERING & TECHNOLOGY

Under

FACULTY COUNCIL OF INTERDISCIPLINARY STUDIES LAW &

MANAGEMENT

JADAVPUR UNIVERSITY

CERTIFICATE OF RECOMMENDATION

I HERE BY CERTIFY THAT THE THESIS PREPARED UNDER MY SUPERVISION BY **SOURADIP PAUL** ENTITLED **LASER BEAM WELDING OF ALUMINIUM ALLOYS** BE ACCEPTED IN THE PARTIAL FULFILLMENT OF THE REQUIREMENTS FOR THE DEGREE OF MASTER OF TECHNOLOGY IN LASER TECHNOLOGY DURING THE ACADEMIC SESSION 2017-2019.

THESIS SUPERVISOR

Dr. Souren Mitra

**Professor, Production Engineering Department
Jadavpur University, Kolkata-700032**

Countersigned

DIRECTOR

Sri. Dipten Misra

**School of Laser Science and Engineering
Jadavpur University, Kolkata-700 032**

DEAN

**Faculty of Interdisciplinary Studies, Law and Management
Jadavpur University, Kolkata-700 032**

JADAVPUR UNIVERSITY
FACULTY OF INTERDISCIPLINARY STUDIES, LAW AND MANAGEMENT

CERTIFICATE OF APPROVAL **

This foregoing thesis is hereby approved as a creditable study of an engineering subject carried out and presented in a manner satisfactory to warrant its acceptance as a pre-requisite to the degree for which it has been submitted. It is understood that by this approval the undersigned do not necessarily endorse or approve any statement made, opinion expressed or conclusion drawn therein but approve the thesis only for the purpose for which it has been submitted.

**COMMITTEE OF FINAL EXAMINATION
FOR EVALUATION OF THESIS**

** Only in case the recommendation is concurred

DECLARATION OF ORIGINALITY AND COMPLIANCE OF
ACADEMIC ETHICS

The author hereby declares that this thesis contains original research work by the undersigned candidate, as part of his **Master of Technology in Laser Technology** studies during academic session 2017-2019.

All information in this document has been obtained and presented in accordance with academic rules and ethical conduct.

The author also declares that as required by this rules and conduct, the author has fully cited and referred all material and results that are not original to this work.

NAME: SOURADIP PAUL

EXAMINATION ROLL NUMBER: M4LST19008

THESIS TITLE: LASER BEAM WELDING OF ALUMINIUM ALLOYS

SIGNATURE:

DATE:

ACKNOWLEDGEMENT

The author has taken immense pleasure to express his sincere gratitude to everyone who has helped him to complete this thesis. First and foremost, the author is deeply grateful to his thesis supervisor Dr. Souren Mitra, Professor, Department of Production Engineering, Jadavpur University for his valuable suggestions, guidance and constant inspiration throughout the period of the thesis work.

The author is grateful to Sri. Dipten Misra, Director, School of Laser Science and Engineering, Jadavpur University for his valuable suggestion during the period of thesis work.

The author has been grateful to Smt. Aparna Sudha Kiran, PhD Research Scholar, School of Laser Science and Jadavpur University for her constant support and guidance throughout the period of thesis work.

The author would like to thank Sri Kingsuk Pal, staff member of School of Laser Science and Engineering, Jadavpur University and Sri Rabi Shankar Pramanik, staff member of Production Engineering Department for his assistance towards the completion of this thesis work.

The author would like to thank Dr. Somnath Paul, Dr. K. Paramsviam for their support and cooperation in completing the thesis work. The author would also like to thank Prithwiraj Roy, PhD. Research Scholar of Production Engineering Department, Jadavpur University and Sri Swagatam Paul, PhD. researcher of Mechanical Engineering Department, Jadavpur University for their cordial cooperation.

The author also would like to thank Sri Soumyabrata Chakravarty, Sri Subha Nath, Sri Indranuj Lahiri, Sri Akashdip Nath, Sri Debmalya Halder and Sri Nandakishor Maity for their valuable moral support.

Lastly but obviously not the least I would like to pay my special admiration thanks to my parents for their constant support, love and faith.

My eternal gratitude goes to God.

SOURADIP PAUL
Examination Roll No. M4LST19008
Registration No. 141049 of 2017-2018

LIST OF FIGURES

Page no.

Fig. 1.1: Schematic representation of the laser welding setup	12
Fig. 2.1: Block diagram of laser welding unit	18
Fig.2.2: Different Modes of welding	19
Fig.2.3 :Schematic diagram of Nd:YAG laser	21
Fig.2.4 :Schematic diagram of CO ₂ laser	22
Fig.2.5:Schematic diagram of fiber laser	22
Fig. 2.6: Lap joint	23
Fig. 2.7: Butt joint	23
Fig.2.8: T joint	24
Fig. 2.9: Tensile testing of welded sample	28
Fig.2.10: Bending test of welded sample	29
Fig.2.11: Hardness testing of welded sample	30
Fig. 2.12 : Porosity in laser welded sample	31
Fig.2.13: Solidification cracking in laser welded sample	32
Fig.2.14: HAZ liquation crack in laser welded sample	32
Fig.2.15: Inclusionin laser welded sample	33
Fig.2.16 : Undercut in laser welded sample	34
Fig.2.17: Underfill in laser welded sample	34
Fig. 3.1 : Laser Beam profile	37
Fig. 3.2 : Laser welding machine	39
Fig. 3.3: Main menu of the laser source machine	40
Fig. 3.4: Welder mode of the laser source machine	41
Fig. 3.5: System work status of laser source machine	41
Fig. 3.6 : Chiller unit	42

Fig. 3.7: Optical microscope	42
Fig. 3.8: Pictorial view of universal testing machine	43
Fig. 3.9 : Pictorial view of lap welding OF Aluminium 2024 alloy	44
Fig. 3.10: pictorial view of butt welding set up	44
Fig. 3.11 : Laser welded lap joint	49
Fig. 3.12: Main effect plots for bond width	49
Fig. 3.13: Bond with vs peak power,frequency	50
Fig. 3.14: Bond width vs scanning speed, frequency	51
Fig. 3.15: Bond width vs peak power, scanning speed	51
Fig. 3.16: Contour plot of bond width vs peak power, scanning speed	52
Fig. 3.17: Contour plot of bond width vs peak power, frequency	52
Fig. 3.18: Contour plot of bond width vs frequency, scanning speed	52
Fig. 3.19: Main effect plots for breaking load	53
Fig. 3.20: Breaking load vs peak power, scanning speed	54
Fig. 3.21: Breaking load vs peak power,frequency	54
Fig. 3.22: Breaking load vs scanning speed, frequency	55
Fig. 3.23: Contour plot of breaking load vs peak power, scanning speed	56
Fig. 3.24: Contour plot of breaking load vs peak power, frequency	56
Fig. 3.25: Contour plot of breaking load vs frequency, scanning speed	56
Fig. 3.26: Main effect plots for theoretical throat length	57
Fig. 3.27: Theoretical throat length vs peak power, scanning speed	58
Fig. 3.28: Theoretical throat length vs peak power, frequency	58
Fig. 3.29: Theoretical; throat length vs scanning speed, frequency	59
Fig. 3.30: Contour plot of theoretical throat length vs peak power, scanning speed	59
Fig. 3.31: Contour plot of theoretical throat length vs peak power, frequency	60

Fig. 3.32: Contour plot of theoretical throat length vs frequency, scanning speed	60
Fig 3.33: Butt welded joint	62
Fig 3.34: Main effects plot for welding width	62
Fig 3.35: Pareto chart of the standardized effects of welding width	63
Fig 3.36: Welding width vs peak power, scanning speed	64
Fig 3.37: Welding width vs peak power, frequency	64
Fig 3.38: Welding width vs. welding width, pulse width	65
Fig 3.39: Welding width vs. scanning speed, frequency	65
Fig 3.40: Welding width vs. scanning speed, pulse width	66
Fig 3.41: Welding width vs. frequency, pulse width	66
Fig 3.42: Contour plot of welding width vs peak power, scanning speed	67
Fig 3.43 : Contour plot of welding width vs peak power, frequency	67
Fig 3.44 : Contour plot of welding width vs peak power, pulse width	67
Fig 3.45: Contour plot of welding width vs scanning speed, frequency	68
Fig 3.46 : Contour plot of welding width vs scanning speed, pulse width	68
Fig 3.47 : Contour plot of welding width vs frequency, pulse width	68
Fig 3.48 : Crack present in welded butt joint specimens	69
Fig 3.49 Pores present in the laser welded butt joint specimens	70

LIST OF TABLES

Page no.

Table 1.1. Classification of wrought aluminum alloys according to their strengthening mechanism	3
Table 1.2. Composition and typical applications of non heat-treatable wrought alloys	8
Table 1.3. Composition and typical applications of heat treatable wrought aluminum alloys	9
Table 3.1. AA 2024, nominal chemical composition (wt.%).	38
Table 3.2. Specification of pulsed laser welding machine	40
Table 3.3. Levels of parameters for lap joint experiment	45
Table 3.4. Design of experiment of laser lap joint experiment	46
Table 3.5. Levels of parameters for butt joint experiment	46
Table 3.6. Design of experiment of laser butt welding	47
Table 3.7. Results of lap welding experiments	48
Table 3.8. Results of butt welding experiments	61

SYNOPSIS

Aluminium alloys are widely used in aircraft industry which involves a large number of joint configurations, traditionally fabricated by riveting. Disadvantages of riveting are extra weight to the structure, stress concentration, crevices corrosion and loosening due to vibrations. Moreover, it is a time consuming and manpower intense task. Laser welding can be a potential tool which is superior to other joining techniques, such as, arc welding due its heat input nature and related microstructural effect. The present study is focused on improving weldability of aluminium alloy 2024 by using a pulsed laser mode. Initially, screening experiments were performed to enumerate the power density requirement for proper coupling of the laser beam in Gaussian, setting the pressure of shielding gas (Ar) which can yield stable keyhole, smooth weld surface. From the butt welded specimen, weldability of the alloy was studied in terms of weld width, cracks and pores. From the lap joint welded specimen, weldability of the alloy was studied in terms of weld width, throat thickness and breaking load. The maximum bond width that was obtained at a peak power of 4.79 kW scanning speed 1.5mm/s and a frequency of 8Hz and theoretical throat length obtained is 983.34 μm which is also obtained at the parameters that gave maximum bond width were calculated. The parameters at which highest breaking load is attained were also checked. The weld parameters in butt joint which yielded lesser pores and cracks were studied.

TABLE OF CONTENTS

Title	Page No.
Title Sheet	
Certificate of Recommendation	
Certificate of Approval	
Acknowledgement	
List of figures	
List of tables	
Synopsis	
1. Introduction	1
1.1 Motivation	1
1.2 Aluminium & aluminium alloys	2
1.2.1 Properties of aluminium alloys	6
1.2.2 Applications of aluminium alloys	7
1.3 Welding	11
1.3.1 Laser welding	12
1.4 Advantages and limitations of laser welding	12
1.4.1 Advantages of laser welding	12
1.4.2 Limitations of laser welding	13
1.5 Survey of past research	13
1.6 Objective of the present research	16
2. FUNDAMENTALS OF LASER BEAM WELDING	18
2.1 Scheme of laser welding	18
2.1.1 Types of laser welding	19

2.1.2	Laser Source used for welding	20
2.1.3	Laser welded joints	23
2.2	Laser welding parameters	24
2.3	Evaluation of quality of laser welded joints	27
2.3.1	Determination of joint strength of welded specimen	28
2.3.1.1	Tensile test	28
2.3.1.2	Bending test	28
2.3.1.3	Hardness test	29
2.3.2	Laser welding defects	30
2.4	Different modes of laser welding	35
2.4.1	Pulsed mode of laser welding	35
2.4.2	Continuous mode of laser welding	35

3. EXPERIMENTAL INVESTIGATION OF LASER BEAM WELDING OF ALUMINIUM ALLOY

3.1	Material composition	38
3.2	Sample preparation	38
3.3	Experimental set up	38
3.3.1	Pulsed laser welding machine	38
3.3.2	Optical microscope	42
3.3.3	Universal testing machine	43
3.4	Experimental procedure	43
3.4.1	Laser welding of lap joint	43
3.4.2	Laser welding of butt joint	44
3.5	Experimental investigation on laser beam welding of aluminium alloy	45

3.5.1	Experimental plan	45
3.5.2	Analysis of experimental results of lap joint	48
3.5.2.1	Results	48
3.5.2.2	Effect of process parameters on bond width	49
3.5.2.3	Effect of process parameters on breaking load	53
3.5.2.4	Effect of process parameters on throat length	57
3.5.3	Analysis of experimental results of butt joint	60
3.5.3.1	Results	60
3.5.3.2	Effect of process parameters on welding width	62
3.5.3.3	Analysis of cracks and pores	69
4.	GENERAL CONCLUSION AND FUTURE SCOPE	71
4.1	General conclusion	71
4.2	Future scope	72
	References	73

CHAPTER 1

INTRODUCTION

1.1. MOTIVATION

Global warming, environment pollution are the major concerns of the society today. Many stringent norms are being imposed on the automobile emission, leading to Bharat 6 which was announced recently. Other than emission reduction, fuel consumption is also a concern to be addressed for the automobile, aerospace and other relevant industries. The demand for vehicles that consume less fuel, flights that charge less, goods that are available at lesser rate are always in demand. Hence the transportation industry is looking for options that help them satisfy the customer. It has been noted that the average weight of the vehicle is in increasing trend since 1970s. This weight increase can be explained by the added safety and comfort equipment as well as the customer demand for higher performance levels and bigger cars. But research shows that for reducing the exhaust pipe carbon dioxide emissions a reduction of the vehicle weight is mandatory, as this provides one of the highest fuel saving possibilities. A weight reduction can be achieved by substituting the heavier materials by lighter and stronger materials, the introduction of new design and manufacturing concepts or ideally by a combination of both. Steel is already paving way to Aluminium alloys are in many automotive applications. The main reason for this is their high strength-to-density ratio, Aluminium alloys possess a density, which is approximately one-third of that of steel, whereas their strength is maximal one-half of that of steel. Consequently, the specific strength of some aluminium alloys, such as Al-Zn alloys, can even exceed the values for ultrahigh strength steels according to Ashby's material selection criterion. These alloys possess a medium to high strength in combination with good formability as well as a good corrosion resistance and weldability.

Although aluminium alloys are accounted with the highest strength, there is no widespread use of these alloys. The reason can be appended to the poor weldability of the alloys owing to their physical properties. Nowadays, laser beam welding belongs to the most efficient welding methods among the fusion welding processes. This can be explained by the high viable welding speeds, the beneficial depth-to-width ratio of the welds and the low heat exposure of the part. This is facilitated by high laser beam powers in combination with small laser beam dimensions, which result in a high energy density. Furthermore, laser beam

welding also enables light-weight part designs due to the small weld dimensions and the low distortion as well as the improved accessibility for contact-free welding. This may lead to further weight reductions of the vehicles. Hence, it can be said that there is a large potential for reducing the weight of vehicles and thereby to meet the challenges of future car regarding fuel consumptions and emissions by the use of Al alloys as light-weight and high-strength materials in combination with laser beam welding as an efficient joining method for the manufacturing of automotive parts.

1.2 ALUMINIUM AND ALUMINIUM ALLOYS

Aluminium is a white metal produced mainly by electrical process from the oxide (alumina), which is prepared from a clayey mineral called bauxite. The great combination of properties of aluminium and its alloys make it one of the most versatile, economical and attractive metallic alloys for a broad range of uses – from soft, highly ductile wrapping foil to the highly demanding engineering applications. After steel aluminium alloys are second in use as a structural metal.

Aluminum alloys can be divided mainly into two major categories: wrought compositions and cast compositions. A further differentiation for each category is based on the primary mechanism of property development. Many alloys respond to thermal treatment based on phase solubilises. These treatments include solution heat treatment, quenching, and precipitation, or age, hardening. For either casting or wrought alloys, such alloys are described as heat treatable. A large number of other wrought compositions rely instead on work hardening through mechanical reduction, usually in combination with various annealing procedures for property development. These alloys are referred to as work hardening. Some casting alloys are essentially not heat treatable and are used only in as-cast or in thermally modified conditions unrelated to solution or precipitation effects.

Cast and wrought alloy nomenclatures have been developed.. The alloy identification system employs different nomenclatures for wrought and cast alloys, but divides alloys into families for simplification. For wrought alloys a four-digit system is used to produce a list of wrought composition families as follows:

- a. 1xxx: Controlled unalloyed (pure) composition, used primarily in the electrical and chemical industries
- b. 2xxx: Alloys in which copper is the principal alloying element, although other elements, notably magnesium, may be specified. 2xxxseries alloys are widely used in

aircraft where their high strength (yield strengths as high as 455 MPa, or 66 ksi) is valued.

- c. 3xxx: Alloys in which manganese is the principal alloying element, used as general-purpose alloys for architectural applications and various products
- d. 4xxx: Alloys in which silicon is the principal alloying element, used in welding rods and brazing sheet
- e. 5xxx: Alloys in which magnesium is the principal alloying element, used in boat hulls, gangplanks, and other products exposed to marine environments
- f. 6xxx: Alloys in which magnesium and silicon are the principal alloying
- g. elements, commonly used for architectural extrusions and automotive components
- h. 7xxx: Alloys in which zinc is the principal alloying element (although other elements, such as copper, magnesium, chromium, and zirconium, may be specified).used in aircraft structural components and other high-strength applications. The 7xxx series are the strongest aluminum alloys, with yield strengths ≥ 500 MPa (≥ 73 ksi) possible.
- i. 8xxx: Alloys characterizing miscellaneous compositions. The 8xxx series alloys may contain appreciable amounts of tin, lithium, and/or iron.
- j. 9xxx: Reserved for future use

Wrought alloys that constitute heat-treatable (precipitation-hardenable) aluminum alloys include the 2xxx, 6xxx, 7xxx, and some of the 8xxx alloys. The various combinations of alloying additions and strengthening mechanisms used for wrought aluminum alloys are shown in Table 1.1.

Table 1.1: Classification of wrought aluminum alloys according to their strengthening mechanism

Alloy system	Aluminum series
Work-hardenable alloys	
Pure Al	1xxx
Al-Mn	3xxx
Al-Si	4xxx
Al-Mg	5xxx
Al-Fe	8xxx
Al-Fe-Ni	8xxx
Precipitation-hardenable alloys	
Al-Cu	2xxx
Al-Cu-Mg	2xxx
Al-Cu-Li	2xxx
Al-Mg-Si	6xxx
Al-Zn	7xxx
Al-Zn-Mg	7xxx
Al-Zn-Mg-Cu	7xxx
Al-Li-Cu-Mg	8xxx

Casting compositions are described by a three-digit system followed by a decimal value. The decimal .0 in all cases pertains to casting alloy limits. Decimals .1, and .2 concern ingot compositions, which after melting and processing should result in chemistries conforming to casting specification requirements. Alloy families for casting compositions include the following:

Aluminum and Aluminum Alloys :

- a. 1xx.x: Controlled unalloyed (pure) compositions, especially for rotor manufacture
- b. 2xx.x: Alloys in which copper is the principal alloying element. Other alloying elements may be specified.
- c. 3xx.x: Alloys in which silicon is the principal alloying element. The other alloying elements such as copper and magnesium are specified. The 3xx.x series comprises nearly 90% of all shaped castings produced.
- d. 4xx.x: Alloys in which silicon is the principal alloying element.
- e. 5xx.x: Alloys in which magnesium is the principal alloying element.
- f. 6xx.x: Unused
- g. 7xx.x: Alloys in which zinc is the principal alloying element. Other alloying elements such as copper and magnesium may be specified.
- h. 8xx.x: Alloys in which tin is the principal alloying element.
- i. 9xx.x: Unused

The properties and performance of a welded joint in aluminum are influenced by many factors, including the composition, form, and temper of the base metals, the filler metal used, the welding process, rate of cooling, joint design, post weld mechanical or thermal treatments, and the service environment.

Metallurgical effects

The effect of the heat of welding, which causes the softening of the base metal adjacent to the weld, is generally the controlling factor relative to the as-welded strength of an aluminium weldment. The composition and structure of the weld metal can also significantly affect final strength, ductility, and toughness.

Weld Metal

The properties of the deposited aluminum weld metal are influenced by the composition and rate of solidification. The solidification rate depends on the welding process and technique, in

addition to all the factors affecting heat input and the rate of heat transfer away from the weld pool. A higher rate of solidification generally produces a finer-grained microstructure with greater strength and decreased tendency for hot cracking.

The composition of the weld metal depends on the chemical composition of the base metal and filler metal, and the resultant mixture is influenced by the joint design, welding process, and procedure employed. When welding the non heat-treatable aluminum alloys, a filler metal with a chemical composition similar to that of the base metal is generally selected. The melting range of the heat-treatable aluminum alloys is much wider and these alloys are more sensitive to hot cracking.

A dissimilar filler metal with a lower solidus temperature than that of the base metal is generally employed; this will allow the heat-treatable base metal completely solidify and develop strength along the fusion zone before weld solidification shrinkage stresses occur.

The molten weld metal exhibits a high solubility for hydrogen. Hydrogen can be introduced into the weld metal from residual hydrocarbons or hydrated oxides on the surfaces of the base and filler metals, and also from faulty welding equipment or improper gas shielding that permits moist atmospheric contamination.

During solidification of the weld, hydrogen precipitates out of the solidifying molten aluminum and becomes entrapped in the solid weld metal as porosity. Thus, it becomes very important to eliminate sources of hydrogen from the weld area when using welding procedures that result in rapid solidification of the weld metal. Bare filler wire must be properly cleaned and stored in a dry environment until needed for production.

Heat-Affected Zone

The effect of the heat of welding on aluminum base alloys varies with the distance from the weld and maybe divided roughly into areas that are represented by the temperature attained by the metal. The length of time at a specific temperature can be significant for the heat-treatable alloys. The width of the heat-affected zone (HAZ) in all alloys and the extent of metallurgical changes in the heat-treatable alloys depend on the rate of heat input and heat dissipation. These are influenced by the welding process, the thickness or geometry of the workpiece, the speed of welding, the preheat and interface temperatures, and the types of backing or fixturing. The strength of the HAZ will be similar to that of the annealed material because the portion of the HAZ subjected to temperatures higher than the annealing temperature will be instantaneously annealed. Time at temperature and cooling rate are not critical variables for these alloys. The service performance of the weldment when

stressed parallel to the weld will depend somewhat on the ratio of the width of the HAZ relative to that of the unaffected base metal. When stressed transverse to the weld, the mechanical properties obtained are independent of the welding process and technique employed in making the weld.

1.2.1 PROPERTIES OF ALUMINIUM ALLOYS

The density of the aluminium is 2.7 gm/ cm^3 which is very much lower than the steel. With such lighter weight some of the alloy of aluminium give very high strength resulting in increase of strength weight ratio, for which it permits design of strong, lightweight structures. Aluminium is very much useful generally for the moving objects where lighter weight is needed such as space vehicles and aircraft and also for land and water-borne vehicles.

Aluminium resist the kind of progressive oxidisation which occurs in steel which rusts away. The outer exposed surface of aluminium reacts with oxygen to make a very thin layer aluminium oxide which is inert and blocks further oxidisation. Aluminium oxide tightly stuck to the original metal and do not flake like iron rust.

If aluminium is properly alloyed and treated it gives resistance against corrosion by water, salt, a variety of chemical and physical agents and many environmental factors.

Aluminium is a highly reflective material. Radiant energy, visible light, radiant heat and electromagnetic waves are efficiently reflected. Due to its high reflectivity, reflectance of a polished aluminium can be used in variety of decorative and functional purposes.

Aluminium is generally has high electric and thermal conductivity except some alloys which are developed with high degree of electrical resistivity. On an equivalent weight basis aluminium gives nearly twice electrical conductivity than copper. Because of high electrical conductivity, low weight and good mechanical strength it is used in long line, high voltage transmission cable. And thermal conductivity is almost half of copper, for this reason it is advantageous in evaporators, heat exchangers, electrically heated appliances and radiators.

Aluminium is non-ferromagnetic. For this property aluminium has importance in electrical and electronics industries.

Aluminium is also non-pyrophoric, for this aluminium is important in applications which are involved in inflammable and explosive materials handling.

It is non toxic material. For this reason it is used in making of food container and beverages.

Aluminium can be fabricated into various forms easily due to its lower degree of workability. The cost of the aluminium is also very cheap. It can be cast and rolled to desirable formation with ease. Aluminium sheets can be stamped, spun, drawn or rolled formed. Aluminium wire can be drawn from rolled rod to desired shape and size. Almost every possible formation can be achieved by the aluminium.

1.2.2 APPLICATIONS OF ALUMINIUM ALLOYS

Due to advantages of different good properties aluminium has several applications everywhere. Conductors in either the 1000 or 6000 series alloys are sensible technical alternatives to copper for all electrical conductors, even in domestic wiring. A very large proportion of overhead, high voltage, power lines utilize aluminium rather than copper as the conductor on weight grounds. The relatively low strength of these grades requires that they be reinforced by including a galvanized or Aluminium coated high tensile steel wire in each strand.

Due its advantages of weight strength ratio aluminium is the prime material in aircraft and high speed car industry. Aluminium gives high strength with low weight and comes in a comparatively low cost, which is very much beneficial for these industries.

Aluminium alloys are also has its application in packaging industry. Some aluminum alloys are being used as foil for food wrapping and for containers utilizes their good corrosion resistance and barrier properties against UV light, moisture and odors. Foil can be readily formed, attractively decorated and can be usefully combined with paper and plastic if required.

In architecture and building, aluminium has a significance application. Aluminium is used in buildings for a wide spectrum of applications. These include roofing for factories which incorporate foil vapor barriers, windows and pre formed sheet cladding features, doors, canopies and fronts for shops and prestigious buildings, architectural hardware and fittings, rainwater goods and replacement windows. Aluminium structures and cladding are also used to refurbish many of the concrete structures built. Aluminium structures and cladding are also used to refurbish many of the concrete structures built.

Except these main application fields aluminium also used in others application to make sports goods, high pressure gas cylinder, road barrier and signs, domestic furniture etc.

Application of different aluminium alloys are tabulated in table 1.2 below

Table 1.2 : Composition and Typical Applications of Non heat -Treatable Wrought Alloys

Aluminum Association designation	Nominal composition (% alloying element)				Typical applications
	Cu	Mn	Mg	Cr	
1060	99.60% minimum aluminum				Chemical process equipment, tanks, piping
1100	99.00% minimum aluminum				Architectural and decorative applications, furniture, deep drawn parts, spun hollow ware.
1350	99.50% minimum aluminum				Architectural and decorative applications, furniture, deep drawn parts, spun hollow ware.
3003	0.1 2	1.2	–	–	Electrical conductor wire, bus and cable.
3004	–	1.2	1.0	–	General purpose applications where slightly higher strength than 1100 is required. Process and food handling equipment, chemical and drums and tanks.
5005	–	–	10.8	–	Sheet metal requiring higher strength than 3003.
5050	–	–	1.4	–	Electrical conductor and architectural applications.
5052,5652	–	–	2.5	–	Similar to 3003 and 5005 but stronger, has excellent finishing qualities.
5083	–	0.7	4.4	0.15	Sheet metal applications requiring higher strength than 5050. Formable and good corrosion resistance. Storage tanks, boats, appliances. Alloy 5652 has closer control of impurities for H ₂ O ₂ service.
5086	–	0.45	4.0	0.15	Marine components, tanks, unfired pressure vessels, cryogenics structures, railroad cars, drilling rigs.
5154,5254	–	–	3.5	0.25	Marine components, tanks, tankers, truck frames.
5454	–	0.8	2.7	0.12	Structural applications and tanks for sustained high-temperature service.
5456	–	0.8	5.1	0.12	Structures, tanks, unfired pressure vessels, marine components.

Table 1.3: Composition and typical Application of heat treatable wrought Aluminum Alloys

Base alloy	Nominal composition (% alloying element)							Typical applications
	Cu	Si	Mn	Mg	Zn	Ni	Cr	
2014	4.4	0.8	0.8	0.5	–	–	–	Structures, structural and hydraulic fittings, hardware and heavy duty forgings for aircraft and automotive uses
2017	4	0.5	0.7	0.6	–	–	–	Same as 2014, screw machine parts
2024	4.4	–	0.6	1.5	–	–	–	Structural, aircraft sheet construction, truck wheels
20036	2.6	–	0.25	0.45	–	–	–	Automotive body sheet
2090	2.7	–	–	–	–	–	–	Structural, high strength and damage tolerant aerospace application
2218	4	–	–	1.5	–	2	–	Forging alloy, engine cylinder heads, pistons, parts requiring for good strength and hardness at elevated temperature
2219	6.3	–	0.3	–	–	–	–	Structural, high temperature strength, aerospace tanks

2519	5.8	–	0.3	0.17	0.06	–	–	Structural, high strength armor
2618	2.3	0.18	–	1.6	–	1	–	Same as 2218
6005	–	0.8	–	0.5	–	–	–	Structural and architectural
6009	0.4	0.8	0.5	0.6	0.25	–	0.1	Automotive body sheet
6010	0.4	1	0.5	0.8	0.25	–	0.1	Automotive body sheets
6013	0.9	0.25	0.35	0.95	–	–	–	General structural application, improved strength over 6061
6061	0.25	0.6	–	1	–	–	0.2	Structural, architectural, automotive, railway and marine application, pipe and pipe settings
6063	–	0.4	–	0.7	–	–	–	Pipe, railings, hardware, architectural application
6070	–	1.4	–	0.8	–	–	–	Structural application, piping
6101	0.5	–	–	0.6	–	–	–	Electrical conductors
6262	0.28	–	–	1	–	–	0.09	Screw machine products, fittings
6351	–	1	0.6	0.6	–	–	–	Same as 6061
6951	–	0.35	–	0.6	–	–	–	Brzing sheet core alloy
7004	–	–	–	1.5	4.2	–	–	Truck trailer, railcar extruded shapes
7005	–	–	0.45	1.4	4.5	–	0.13	Truck trailer, railcar extruded shapes
7039	–	–	0.3	2.8	4	–	0.2	Armour plate, military bridges

7075	1.6	–	–	2.5	5.6	–	0.23	High strength , aircraft and other applications, cladding gives good corrosion resistance
7079	0.6	–	–	3.3	4.3	–	0.2	Strongest aluminium alloy where section thickness exceeds 76.2 mm, large and massive parts for aircraft and allied construction
7178	2	–	–	2.8	6.8	–	0.23	Aircraft construction, slightly higher strength than 7075

1.3 WELDING

Welding is a joining process by which similar or dissimilar material can be joined with application of heat in the joint. During the process heat is applied at the joint by different ways, the joint portion of both the material got melted and with or without help of filler material they combined with each other and when they solidified, the parts got joined with each other. The result is a continuity of homogeneous material, of composition and characteristics of two parts which are being joined together. Welding quality of a joint depends on the weldability of the material. Weldability has been defined as the capacity of being welded into inseparable joints having definite weld strength, proper structure etc. The weldability depends on five major factors – melting point, thermal conductivity, thermal conductivity, thermal expansion, surface condition and change in micro structure.

Presently there are many methods of welding. Different types of welding are gas welding, arc welding, resistance welding, thermit welding, solid state welding, electron beam welding and laser welding.

1.3.1 LASER WELDING

Laser welding is a fusion joining process that produces coalescence of materials with the heat obtained from a concentrated beam of coherent, monochromatic light impinging on the joint to be welded. In the laser beam welding (LBW) process, the laser beam is directed by flat optical elements, such as mirrors and then focused to a small spot (for high power density) at the workpiece using either reflective focusing elements or lenses.

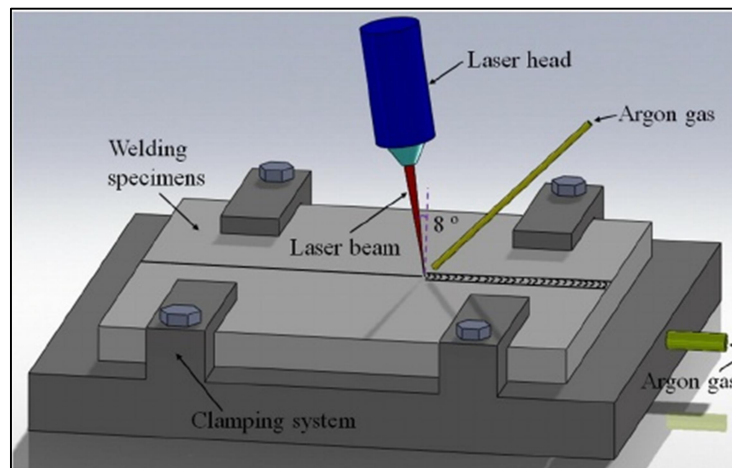


Fig 1.1 Schematic representation of the laser welding setup

1.4 ADVANTAGES AND LIMITATION OF LASER WELDING

1.4.1 ADVANTAGES OF LASER WELDING

Laser welding with a beam power density of 10^4 W/mm² at the work surface is extremely advantageous, often permitting welding speed of several meters per minute and total heat input is much lower than that achieved when arc welding a similar work piece. Added to this, the deep narrow and near parallel laser weld shape, plus very narrow HAZ collectively produced very small work piece distortion.

The deep penetration capability of laser welding allows several layers of material to be lap welded in a single pass. Another advantage is that the weld can usually be placed exactly where it is required very precisely. This aspect has very much important because a weld which joints parts through the full thickness of the mating faces should be strong in both fatigue and tensile strength, as it allows the lines of stress to pass through the joint smoothly.

At the base of the narrow gaps where other welding techniques are inaccessible, laser weld can be successful.

Laser welding speed is high and several work stations can time share one laser. Laser welding are suited for automation and be used in robots. Thus high production rates and flexibility can be achieved with laser welding.

A wide range of similar or dissimilar material joining with can be achieved using laser welding. Material allowance for post weld machining are minimised and weld size is are also very much lower than other techniques. Thus component design opportunities are enhanced in laser welding.

1.4.2 LIMITATIONS OF LASER WELDING

As the beam radius is very low, if the gaps between the joints are not that much low, the beam may pass through it, it will not give proper laser welding, for this reason close fitting and well clamped joints are required, without proper clamping arrangements it will produce poorly fitting parts.

Beam should be properly focused to get the proper power density and and should pass through the line of joint accurately. Else results inaccurate joining.

Precision work piece or beam manipulation equipment is necessary to control energy input.

Compare to the other welding process laser welding machine operating cost is very high. The arrangement cost is also higher. Laser cooling arrangements should be there also/.

Safety should be taken while laser welding. Safety screening around the operating envelope of the laser gun is essential for operator safety. This aspect is difficult to achieve for general on site welding operations.

1.5 SURVEY OF PAST RESEARCH

Many studies have focused on laser welding of aluminium alloys for different joint designs and varying parameters. Techniques of real-time monitoring and process parameters selection, microstructure and numerical simulation etc are topics of interest in the laser welding. This section deals with review of literature on laser welding of aluminium alloys with focus on AA 2xxx, 5xxx, 7xxx series.

Research Progress on Laser Welding of AA 2024-T3

Generally, AA 2024-T3 is considered not weldable by arc welding processes, hence, it has very limited use for welding applications especially in any stress environment. On the other hand, laser welding of aluminium alloys in general, has been performed for many years as early as 1980s.

Huntington and Eagar [3] performed several welding trials on 6.4 mm thick pure aluminium 1100 and 5456 alloy using a CO₂ laser at low laser powers of 0.2 and 1.3 kW. They reported that the joint geometry and surface conditions influence on laser beam absorption significantly. CO₂ lasers have been predominantly used until the late 1990s, when higher power output solid state lasers such as Nd:YAG lasers became available.

Leong *et al.* [4,5] studied the welding parameters necessary to attain consistent laser welds in 5182 and 5754 alloys for automotive applications, using both CO₂ and Nd:YAG lasers.

Zhao *et al.* [6] conducted studies on several series of aluminium alloys namely, 2008, 2010, 5083, 5086, 5251, 5456, 5754, 6013, 6061, 6063, 6082 and 6111 alloys, using both CO₂ laser and Nd:YAG laser and also discussed their applicability in automobile industry. Substantial research has been conducted on CO₂ and Nd:YAG laser welding of 5000 and 6000 series aluminium alloys at least over the last two decades due to their good weldability compared with the crack sensitive 2000 series alloys. However, relatively less work has been reported on laser welding of AA 2024.

Bardin *et al.* [7] employed a 4 kW Nd:YAG laser to weld 13 mm thick AA 2024-T3 in conduction mode and attained only partial penetration.

Hu and Richardson [8] also conducted autogenous welding with 3 mm thick AA 2024 sheets on a 3 kW Nd:YAG laser. The final weld quality was poor with porosity formation due to keyhole instabilities at lower laser heat input. The welding process was observed to be relatively stable at higher heat inputs and the welds has less porosity with smaller keyhole fluctuations. It was concluded that high reflectivity is the main reason for the instability of keyhole. The higher reflectivity raises the threshold of the required power density required

for the welding process and the presence of alloying elements like magnesium owing to their low boiling point which leads to lower mechanical properties.

Snchez Amaya *et al.* [9] conducted a series of experiments on 2mm thick 2024, 5083, 6082 and 7075 in conduction mode with power ranging from 1.5 to 2.75 KW and velocity with variable ranges. It was concluded that crack sensitivity and poor penetration was observed under certain welding conditions.

Alfieri *et al.* [10,11] and Caiazza *et al.* [12] performed experiments on laser welding on a 3.2 mm thick AA 2024 using a disc laser. The importance of proper preparation to improve the weld quality, and beam defocussing to reduce porosity etc were discussed. Tensile strength of welded joints was measured to be greater than 2/3 of the BM and therefore, gave ground for industrial application.

Enz *et al.* [13] explored the fibre laser welding of a dissimilar T-joint made of 2 mm thick AA 2024 and AA 7050, welded by using a 1.2 mm diameter filler metal of AA4047.

Some of the literature concentrated on other series of aluminium include laser welding of 5052 [14], 5083 [14–17], 5356 [18,19], 5754 [20] and 5J32 [21] alloys of the 5000 series; and 6056 [22,23], 6061 [24] and 6156 [25] alloys of the 6000 series. Few other publications also covered welding of 7000 series aluminium alloys such as CO₂ laser welding of 7075 by Liu *et al.* [25], and CO₂ and Nd:YAG 25 laser welding of 7475 by Weston *et al.* and Squillace *et al.* [26,27]. More recently, Chen *et al.* [28] and Cui *et al.* [29] conducted investigated Nd:YAG laser welding of an aluminium lithium alloy, 5A90. Fibre laser welding of AA 2024-T3 is not well understood and requires much to be investigated. Meanwhile, extensive research has been conducted on fibre laser welding of other aluminium alloys. In particular, the 5000 and 6000 series alloys have been studied by many researchers, including AA 6013 [30-37], AA 6061 [38], AA 5052 [39-41], AA 5A06 [42] and AA 5083 [34].

Paleocrassas and Tu [43] investigated low welding speed and low laser power welding of AA 7075 using a 300 W single mode Yb fibre laser for speeds from 1 mm/s to 10 mm/s, which below the minimum speed threshold of 1 mm/s became very unstable due to overheating of the molten pool.

Zhang *et al.* [44,45] studied fibre laser welding of 20 mm thick AA 7075 but using a higher laser power 4 kW fibre laser.

Allen *et al.* [46] used a high power fibre laser for laser welding and hybrid laser-metal inert gas (MIG) welding of 7000 series aluminium alloy of 6 and 12 mm thickness but the exact processing parameters were not stated.

Brown *et al.* [47] used a low power 600 W fibre laser for welding unalloyed AA 1100 and was able to obtain uniform high aspect ratio welds.

Shiganov *et al.* [48] compared welding of a novel Al-Mg-Sc-Zr alloy, the AA 1570 alloy using a 3.5 kW fibre laser and a CO₂ laser for aircraft applications. The use of the fibre laser for welding 2 mm thick AA 1570 increased efficiency by 25-30% in comparison with the CO₂ laser, where the power density required for starting penetration using the fibre laser was around 50% lower than using the CO₂ laser.

Chu *et al.* [49] explored the microstructure, texture and mechanical properties of aluminium alloy 6061. It is reported that the weld width increased continuously with the heat input. Softening of HAZ is observed and all the specimens failed in the mechanical testing showing the characteristics of ductile fracture.

1.6 OBJECTIVES OF THE PRESENT RESEARCH

Research gap/ need identified from the study of past research

The properties of aluminium alloys are responsible for the defects that occur in the welded components. The yield and tensile strengths are much lower for the weld compared to the base material leading to a mismatch of mechanical properties in most of the laser welded aluminium alloys. This disparity is arising due to the defects that form during the laser welding process. Though many theories are postulated about formation of cracks, porosity, underfill etc, the problem still persists leading to less reliable welded joint from aluminium alloys. The reason for the non reliability is appended to the physical properties added to the numerous parameters that influence the welding mechanism. Strict control of the process in the complex environment where the mechanical and metallurgical phenomenon plays an equally important role is always difficult. Hence, efforts are needed to reduce the crack sensitivity of the alloys and thereby increasing the quality of weld.

Hence, the objectives of this present thesis are as follow:

- a) Study the different laser systems and mechanism of laser welding
- b) Experimentation on aluminium alloys for different joint configurations.
- c) Mechanical testing of laser welded aluminium components to find out the maximum tensile they can withstand.
- d) Optical measurement on the aluminium welded components to check width, depth of penetration and the defects present in the welding

CHAPTER 2

FUNDAMENTALS OF LASER BEAM WELDING

2.1 SCHEME OF LASER WELDING

Laser welding is a highly intense welding which can do welding with speed and precision with automation. Laser welding process requires several arrangements to make the welding process efficiently. A block diagram of a complete laser welding unit is given below.

A laser welding unit mainly comprises of three main parts i.e. welding machine, laser source and chiller unit.

A stable power supply is required to provide the energy to these three parts.

Laser is a highly intense power source and radiation of laser can cause several damages to the operator. For this reason a completely sealed environment is required to protect the radiated rays. Welding machine consist of mainly laser torch, work table with a fixture and a led light. For laser welding process choosing proper fixture has a very important role. Laser beam has very small diameter, so if the joint is not properly mated, the beam will not fall on the joint perfectly and even pass through the gap between the joint. When the laser beam impinge on the surface it will creates a force acting on the surface, to prevent the distortion of the material proper work handling fixture is needed.

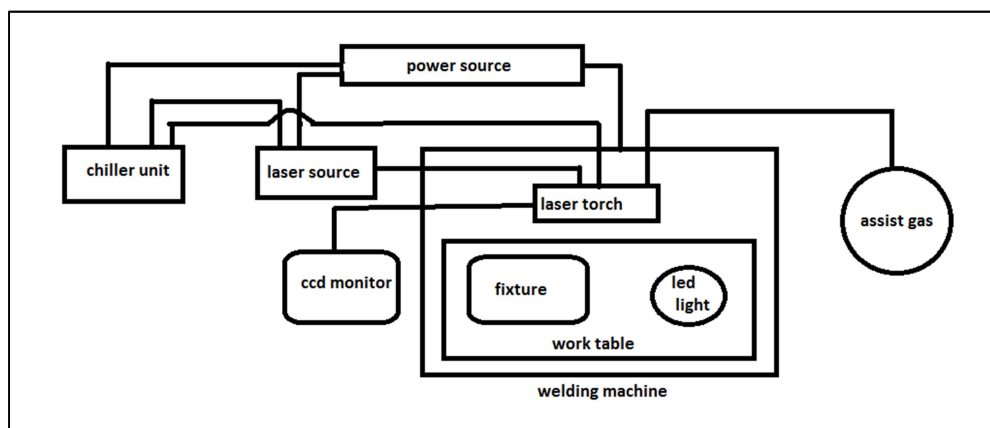


Fig. 2.1 Block diagram of laser welding unit

As a high amount of power is generated during lasing action, one chilling unit should be attached with the laser system to make the temperature normal. Cooling water connection should be attached with laser torch as well as to the laser source.

Laser ray has highest intensity at its focus, so focus measuring instruments is needed to make a laser welding efficiently. For some materials, during laser welding contamination is formed due to presence of atmosphere, to prevent this proper assist gas should be used. Assist gas also helps to cool the joint portion.

With these arrangements laser welding can be done hazardlessly and efficiently.

2.1.1 TYPES OF LASER WELDING

When a laser beam strikes a material which is opaque one portion of the energy gets absorbed and other portion reflected back. The absorbed laser energy can be considered as a point heat source at the surface. Photo electron interaction raises the energy states of the electrons present in the conduction band of the surface material. That increases the temperature of the electron gas and the energy is transferred to the material lattice. Heat transfer from the radiated volume, which is directly heated by the laser beam, to the bulk volume, occurs by conduction mechanisms. As a result intense localized heating of material occurs. If proper power with adequate time is given the surface material can be melted or even boiled. When a laser beam alone is used to fuse the materials to be joined, the process is called autogenous welding. No filler material is used. Depending on the intensity available from the laser source, the welding is carried out in different modes namely, conduction, deep penetration, and keyhole welding. Typical shape of conduction, deep penetration, and keyhole weld cross-sections are shown in Fig.2.2

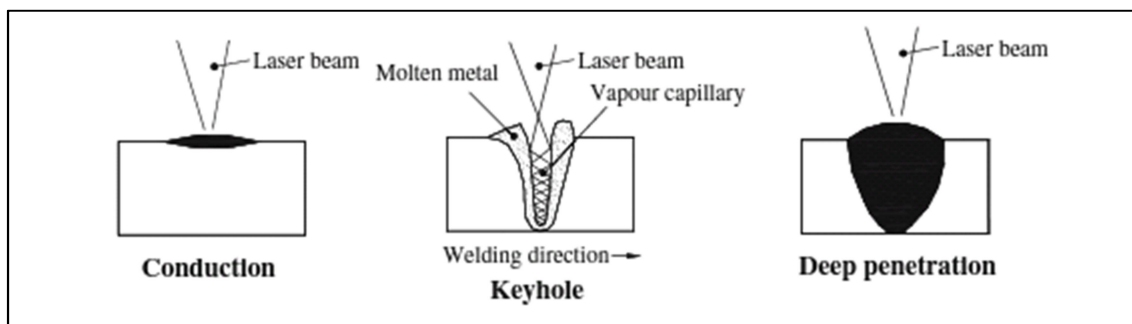


Fig.2.2 Different modes of welding

a) Conduction mode

This mode is guided by the principles of heat conduction. The top surface on which the beam is incident will absorb the heat and it will be conducted into the metal creating a wide weld. The energy density will be low, around $0.5\text{W}/\text{m}^2$. As shown in figure1, The weld nugget formed will be shallow and wide with semi circular and semi spherical profile. The steady state will be attained when there is a balance of heat input and heat lost through conduction. The material will be used by creating a joint with less vaporization.

b) Deep penetration mode

This occurs at the medium power density. The penetration will be deeper than that in the conduction mode. The weld aspect ratio will be one.

c) Keyhole mode

This mode will be carried out at higher intensities. The energy deposited in the weld zone exceeds the energy transferred by conduction or other modes of heat transfer in the work piece. The material gets vaporized creating a dip in the center of the melt pool. A weld pool will be created with molten metal lining it. The surface tension of the molten metal will be different in various locations and the molten metal in the center of the pool tends to flow up deepening the dip until the formation of a through hole. The weld quality depends on the stability of the keyhole and transport of the molten metal from the front towards back by moving around the keyhole.

2.1.2 LASER SOURCES USED FOR WELDING

Lasers can be various types but the lasers which are used predominantly are Nd YAG lasers and CO_2 lasers. Recently high power fiber lasers are also using in some purposes of laser welding.

a) Nd:YAG lasers

Nd : YAG lasers are most used laser which are used for commercial welding purposes. Nd:YAG laser is a solid states laser and It utilizes an impurity in a host material as the active medium. Thus, the neodymium ion (Nd^{+++}) is used as a ‘dopant’, or purposely added impurity in either a glass or YAG crystal and the $1.06\ \mu\text{m}$ output wavelength is dictated by the neodymium ion. The lasing material or the host is in the form of a cylinder of about 150

mm long and 9 mm in diameter. Both ends of the cylinder are made flat and parallel to very close tolerances, then polished to a good optical finish and silvered to make a reflective surface. The crystal is excited by a krypton and Xenon lamp. The generation of high average power in ND:YAG laser system is accomplished by combining several individually pumped laser rods in a single resonator. This optimizes both pumping and extraction efficiency. Oscillator-amplifier configurations also may be used instead of single multirod oscillators. Nd YAG lasers may be operated in three modes, these are continuous output mode, pulsed mode and Q switched mode. Lasers average out power can be 0.3 to 4kW with peak power range is upto 100kW. One of the main advantages of the Nd: YAG laser are they have the ability to deliver laser radiation through optical fibers. Propagation of this laser radiation over several hundred meters is possible with minimal loss.

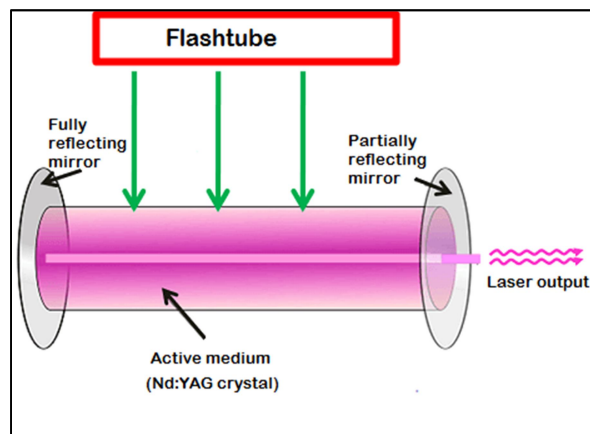


Fig.2.3 Schematic diagram of Nd:YAG laser

b) CO₂ laser

This is gas laser. Though Nd YAG laser are the most applicable laser for welding, the CO₂ laser remains workhorse of industrial laser welding system because it is simple and reliable and is available as a robust well engineered industrial machine. These lasers employ gas mixtures primarily containing nitrogen and helium along with a small percentage of carbon dioxide, and an electric glow discharge is used to excite the CO₂ molecules. Gas heating produced in this fashion is controlled by continuously circulating the gas mixture through the optical cavity area. With CW CO₂ lasers can give 5-10 KW output power. The advantages of CO₂ laser are they give high electrical efficiency, the operating cost is also low and they are easily scaled to high powers.

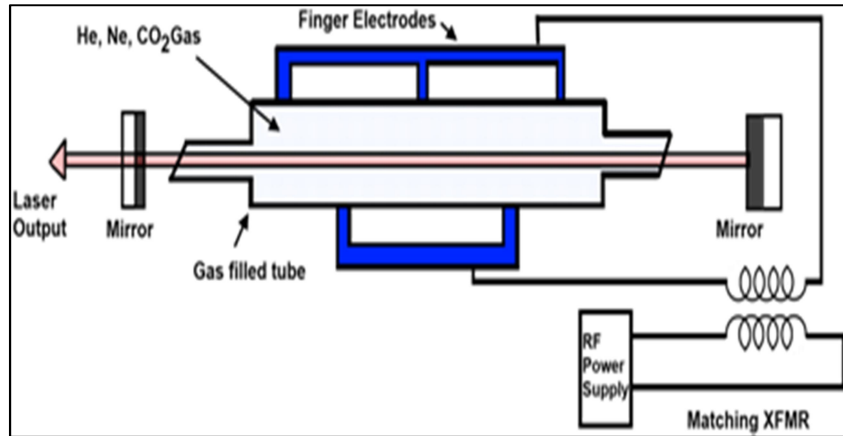


Fig. 2.4 Schematic diagram of CO₂ laser

c) Fiber laser

Besides Nd:YAG and CO₂ laser presently fiber laser also emerging as an option in laser welding field. After high power diode pumped fiber lasers were developed. Fiber lasers have been stated to be a serious alternative to solid state and carbon dioxide lasers for different materials processing applications. In a fiber laser, the active medium is the core of the fiber doped with a rare earth. Most commonly, this is a single-mode fiber laser made of silica. The pump beam is launched longitudinally along the fiber length and it may be guided by either the core itself, as occurs for the single-mode lasers or by an inner cladding around this core. These new lasers have multiple advantages, namely: the high efficiency, compared to lamp or diode pumped rod lasers; the compact design, which simplifies its installation; a good beam quality, due to the use of thin fibers, and thus small beam focus diameter; a robust setup for mobile applications. The scaling of the laser power is achieved by a modular design comprising several single mode lasers.

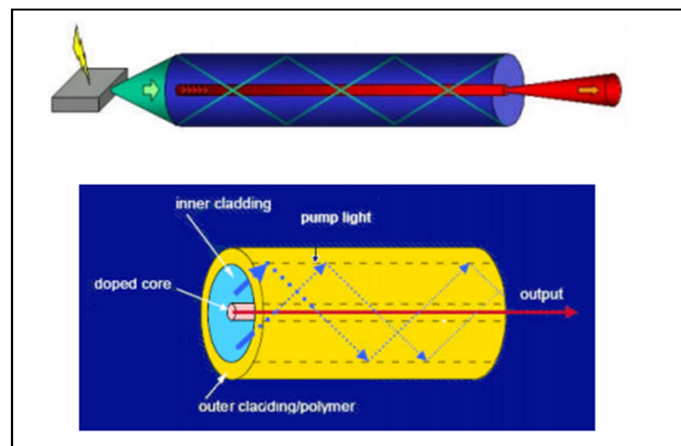


Fig.2.5 Schematic diagram of fiber laser

2.1.3 LASER WELDED JOINTS

Laser welding has the flexibility and can be automated, for this reason many complex types of joint can be done using laser welding. The main joints can be done using laser welding are

a) Lap joint

In this type of joints two metals are overlapped each other to form the joint. Welding can be done on the edges of two sides and if the thickness of the plates are small welding can be done in a distance from the edges in the overlapped portion. This is called lap seam joint. Lap joints give good strength and relatively easier to weld using laser.

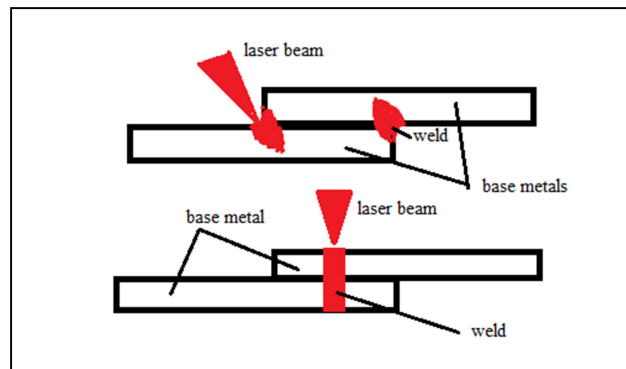


Fig. 2.6 Lap joint

b) Butt joint

In this type of joint two metals should be in a same plane and in their mating portion welding is done. Butt joints are difficult to make using laser welding. For this welding special fixture should be required thus the gap between the metals should be very small. Laser beam diameter is generally very small, so it can pass through it if the gap between the metal is larger than beam diameter. It will create poor welding or no welding at all. Small thickness plates are preferable for this joint.

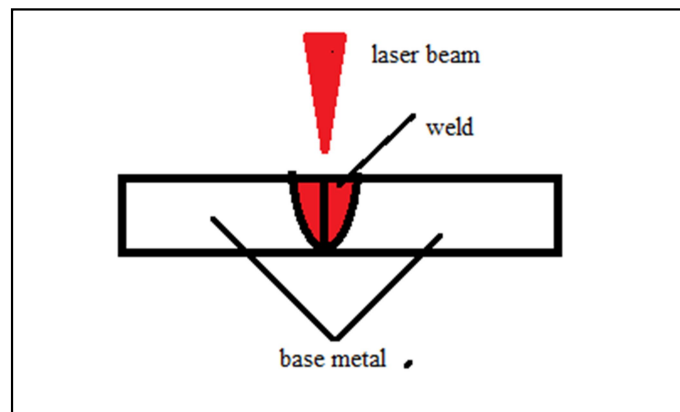


Fig.2.7 Butt joint

c) T joint

In this type of joint two plates are perpendicularly placed and at the joint welding action is done. Depending upon the size and requirements, welding can be done whole circumference of the mating portion or two sides. Fixture is needed to hold the metal perpendicularly to each other. Various kind of T joints can be done depending upon their shape and size.

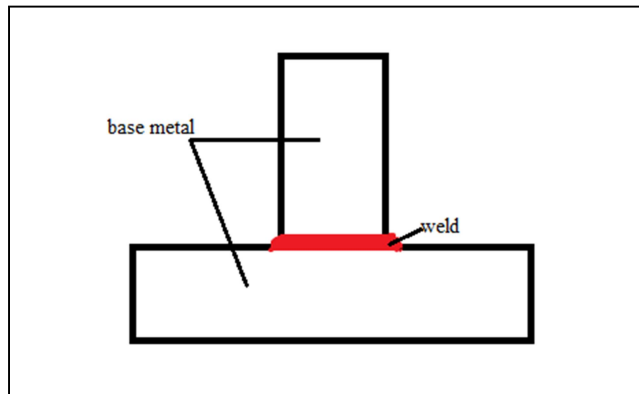


Fig. 2.8 T joint

2.2 LASER WELDING PARAMETERS

Many process parameters affect the properties and quality of the welded component [50].

Parameters that affect the weld quality are

1. Wavelength

For attaining desired weld, the electromagnetic energy of the laser light gets transformed into thermal energy inside the material. This amount of transformation depends on the absorptivity of the material which in turn is influenced by the wavelength. The light of longer wavelength beam is more reflective restricting its usage on aluminium alloys. So, higher threshold power densities are required for coupling with the given material. A beam with shorter wavelength increases the process stability. There will be higher Fresnel absorptivity. The plasma effects are minimum because the absorptive coefficient in the plasma approximately varies with the square of the wavelength.

2. Beam power

This is the most important factor for keyhole formation. For welding the aluminium alloys higher power densities are required because of the higher reflectivity and

thermal conductivity. But, at higher powers the plasma plume could be higher. Higher chances for formation of spatter, undercut, underfill and drop out.

3. Spot size and power density

The power density that is required is decided by the spot size. When the spot size is smaller the power density is higher. The main drawback is that welds will become narrower than necessary or not fused properly. It is recommended to use 30% of the weld width in the range 0.1-1.0mm with 0.3mm being the common one for butt-weld. Small spot size does not ensure good welding performance. In case of overlapping welds the laser spot size is generally set to the desired weld width.

4. Beam divergence

The beam divergence of a laser beam is a measure for how fast the beam expands as it propagates in space. Beam divergence is the derivative of the beam radius with respect to the axial position in the far field. This definition yields a divergence half-angle, and further depends on the definition of the beam radius (or, diameter). Sometimes, full angles are used which results in twice as high angles. Beams with a very small divergence, i.e. with an almost constant beam diameter over a significant propagation distance are generally called “collimated beams”.

5. Focal length

If focal length, the waist diameter and DOF are smaller the divergence angle is larger. Consequently spatter can be generated, the vapour damages the optics etc. Usually, focussing optics have a focal length of 100-200mm

6. Depth of focus

It is the allowable distance the part can deviate from the point of best focus for acceptable weld quality. When welding higher thickness sections, higher DOF is useful.

7. Focal plane position

Focal plane is the plane in which the laser beam waist diameter is minimum. It should be positioned in such a way that the beam can produce maximum depth of penetration with the possibility of best process tolerances.

Focusing above the surface (positive focusing) may result in more plasma and less energy reaching the keyhole. Focusing below the surface (negative focusing) can optimize coupling efficiency as well as increase energy absorption inside the weld pool through multiple reflections. Consequently, the threshold power density is lower for negative focusing compared to positive focusing. By slight defocusing into the work piece, higher depth of penetration and welding speeds also can be achieved.

8. Welding Speed

The depth of penetration increases with the decrease in welding speed. When process speed increases. The depth of keyhole decreases. The weld geometry retains its shape. But, with a decrease in speed, keyhole depth increases only to a particular limit leading to conduction mode of welding. The advantages of high speed welds are: minimum evaporation of alloying elements and fusion zone gets refined grain structure

9. Shield gas

In conventional welding process, inert gas shielding is provided in the weld zone, to avoid oxidation of the weld metal or contamination of the weld metal by adversely affecting materials in the nearby zones such as moisture, oil/grease, or other possible contaminants. However, laser welding has a few advantages over conventional arc welding processes. As the seam widths are small, shielding becomes easier. In autogenous mode, there is no filler wire added eliminating the possibility of contamination, if any, from the filler wire droplets. While welding with higher welding speeds often the shielding gas is exposed to high temperatures about 10000K and get dissociated, ionized, and activated and the extent of their interaction with the weld zone varies with the type of gas, temperatures reached, and the time for which exposed to high temperature. Accordingly, in laser welding, shielding gas has additional functions to be performed, such as, protecting the optic lenses from weld spatter and fumes, suppression of plasma, especially in CO₂ laser wavelength to take care of instabilities of the vapour-filled keyhole, reduced penetration and increased coarse porosity, etc. Poorly shielded weld exhibits porosity, undercut, and bead roughness. With filler metal, weld pool is larger and longer than in autogenous welding, necessitating better shielding.

10. Surface condition

This attains more importance in laser welding compared to conventional welding processes. Laser welding creates a very fast melting rate in the weld and contaminants can create local areas of poor metallurgy, or if the contaminants are volatile, it will create explosive metal loss in the weld. The very low heat input and autogenous nature of the laser welding results in very little molten metal volume to reflow and very little time for that small volume to flow into any flaws. Surface roughness of the work piece and surface contaminants increase absorptivity, While roughening, the surface can be advantageously used, surface contaminants can have adverse effects on weld properties, such as oxide inclusions in steel and porosity in aluminum welds.

11. Joint design and fit-up

Butt and lap-joints are the mostly used designs for laser welding among various possible designs including fillet, coach, standing edge, etc. Because of the highly precise energy beam, joint fit-up attains high importance in laser butt welding. For example, in Nd:YAG laser welding typical tolerances allowed are maximum gap 0.1mm (or 10% of material thickness); focus position ± 1 mm; vertical mismatch < 0.2 mm.

When working in pulsed mode, pulse energy, pulse duration, pulse shape and repetition rate, mean laser power, average peak power and power density also influence the process.

Other influential parameters are welding time and length of weld. Since the incident beam should be absorbed by the material, parameters like thermal conductivity, reflectivity, melting temperature, thickness, heat capacity of the material influence the weld quality

2.3 EVALUATION OF QUALITY OF LASER WELDING JOINTS

A good weld should have a combination of good strength and minimum welding defects. So, determination of these two parameters has important role to determine quality of the weld. Weld joints are generally subjected to destructive tests such as hardness, toughness, bend and tensile test for developing the welding procedure specification and assessing the suitability of weld joint for a particular application. Visual inspection reflects the quality of external

features of a weld joint such as weld bead profile indicating weld width and reinforcement, bead angle and external defects such as craters, cracks, distortion etc. only.

2.3.1 DETERMINATION OF JOINT STRENGTH OF WELDED SAMPLE

To measure the weld joint strength mainly tensile test, bending test and hardness testing can be done.

2.3.1.1 TENSILE TEST

Tensile properties of the weld joints namely yield and ultimate strength and ductility (%age elongation, %age reduction in area) can be obtained either in ambient condition or in special environment (low temperature, high temperature, corrosion etc.) depending upon the requirement of the application using tensile test which is usually conducted at constant strain rate. Tensile properties of the weld joint are obtained in two ways a) taking specimen from transverse direction of weld joint consisting base metal heat affected zone-weld metal-heat affected zone-base metal and b) all weld.

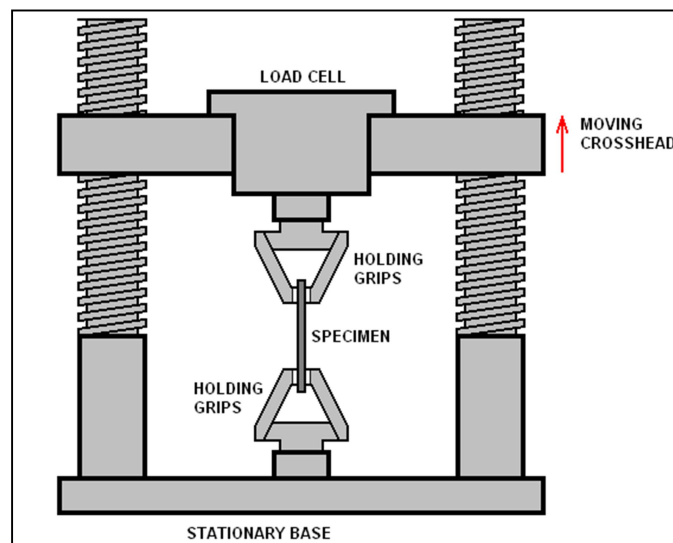


Fig. 2.9 Tensile testing of welded sample

2.3.1.2 BENDING TEST

Bend test is one of the most important and commonly used destructive tests to determine the ductility and soundness (for the presence porosity, inclusion, penetration and other macro-size internal weld discontinuities) of the weld joint produced using under one set of welding

conditions. Bending of the weld joint can be done from face or root side depending upon the purpose i.e. whether face or root side of the weld is to be assessed. The root side bending shows the lack of penetration and fusion if any at the root. Further, bending can be performed using simple compressive/bending load and die of standard size for free and guided bending respectively. Moreover, free bending can be face or root bending while guided bending is performed by placing the weld joint over the die as needs for bending is better and controlled condition as shown in Fig. . For bend test, the load increased until cracks start to appear on face or root of the weld for face and root bend test respectively and angle of bend at this stage is used as a measured of ductility of weld joints. Higher is bend angle (needed for crack initiation) greater is ductility of the weld. Fracture surface of the joint from the face/root side due to bending reveals the presence of internal weld discontinuities if they exist.

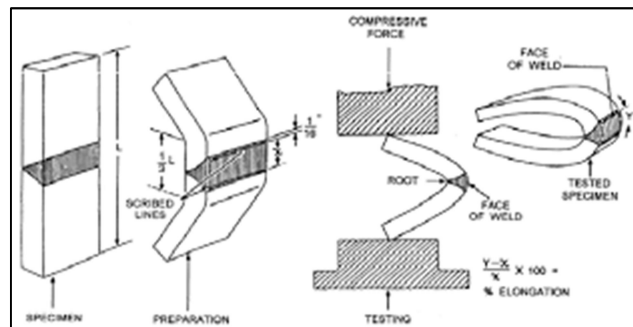


Fig. 2.10 Bending test of welded sample

2.3.1.3 HARDNESS TEST

Hardness is defined as resistance to indentation and is commonly used as a measure of resistance to abrasion or scratching. For the formation of a scratch or causing abrasion, a relative movement is required between two bodies and out of two one body must penetrate/indent into other body. Indentation is the penetration of a pointed object (harder) into other object (softer) under the external load. Resistance to the penetration of pointed object (indenter) into the softer one depends on the hardness of the sample on which load is applied through the indenter. All methods of hardness testing are based on the principle of applying the standard load through the indenter (a pointed object) and measuring the penetration in terms of diameter/diagonal/depth of indentation. High penetration of an indenter at a given standard load suggests low hardness. Penetration due to applied normal load is affected by unevenness on the surface and presence of hard surface films such as oxides, lubricants, dust and dirt etc. if any. Therefore, surface should be cleaned and polished

before hardness test. In case of Brinell hardness test, full load is applied directly for causing indentation for measuring hardness while in case of Rockwell hardness test, minor load (10 kN) is applied first before applying major load. Minor load is applied to ensure the firm metallic contact between the indenter and sample surface by breaking surface films and impurities if any present on the surface. Minor load does not cause indentation. Indentation is caused by major load only. Therefore, cleaning and polishing of the surface films becomes mandatory for accuracy in hardness test results in case of Brinell test method as major load is applied directly.

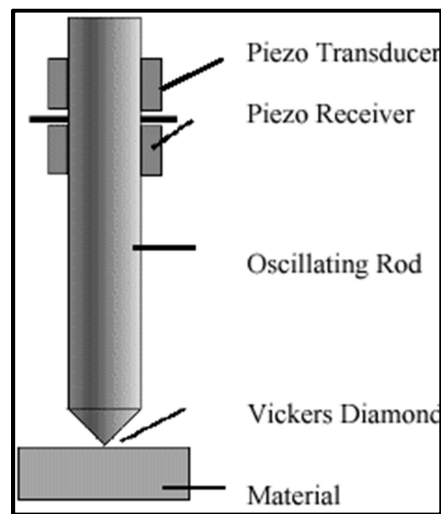


Fig. 2.11 Hardness testing of welded sample

2.3.2 LASER WELDING DEFECTS

A good weld should adequately fulfill all its service requirements. So, while choosing a welding technique it is essential to establish what the welding service requirements will be and whether the chosen welding technique will produce a weld which will achieve them. Welding defects can be many types which can be occurred due to different reasons. Welding defects should be minimised to get a strong and lasting welding. Main types of welding defects are

a) Porosity

Porosity generally occurs when gas bubbles are entrapped in the weld portion during solidification. However, there are other sources which can create porosity such as air intake with moisture into the weld pool. Due to surface contamination from oil, grease or paint can be another source. All of the reasons of porosity can be removed by carefully cleaning of the base material or by some pre experiment surface treatments.

Porosity which are very small compare to the weld depth and which are well dispersed along the weld length do not significantly affect mechanical properties of weld but in presence of large number of porosity, the weld area is reduced results the reduction of weld strength and other mechanical properties. In deep laser welds, in close butt joints, where full penetration is not occurred through thickness is generally prone to porosity. This is due to material outgassing and the bubbles having long escape route, thus before the gas gets out, the keyhole closure occurs and the gas gets entrapped. Where for full penetration keyhole welding the bubbles get option to choose two paths to get out from the weld, so the chance of the bubbles of getting entrapped is reduced. So, the combination of power and welding velocity should be proper to ensure the escape of the bubbles.

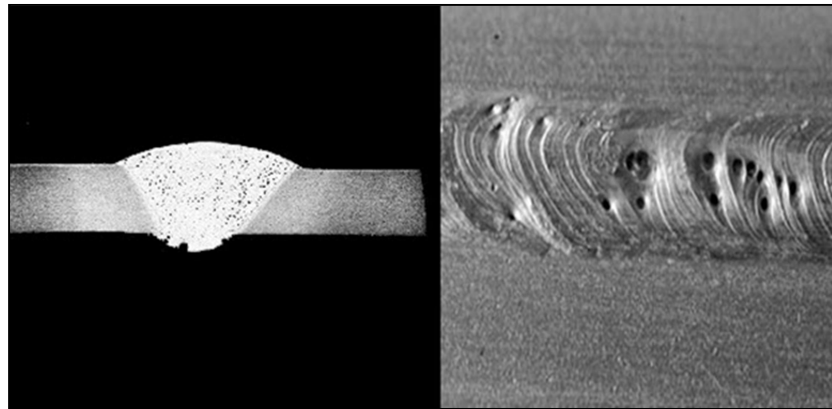


Fig. 2.12 Porosity in laser welded sample

b) Solidification cracking

Solidification cracking occurs at high temperatures above the solidus under circumstances where the material has low ductility and under high contraction stresses.

At a particular temperature point (liquidus) the liquid weld metal starts to solidify and the process continues until a particular lower temperature point (solidus) reaches. Between these two temperatures the alloy element is in a partially solidified state where it is brittle and no ductility until solidus point reaches. This brittleness is present in the films surround the solidifying grains or dendrites and during the solidification when subjected to high transverse contraction stresses, solidification cracking may arise in the film boundaries. Solidification generally occurs near to the centreline of the weld which are suppose to cool at last. If a material prone to

solidification cracking and other suitable material inclusion if not possible, then for this case partial penetration should be avoided and proper joint design should be made to reduce the weld contraction stresses on cooling.

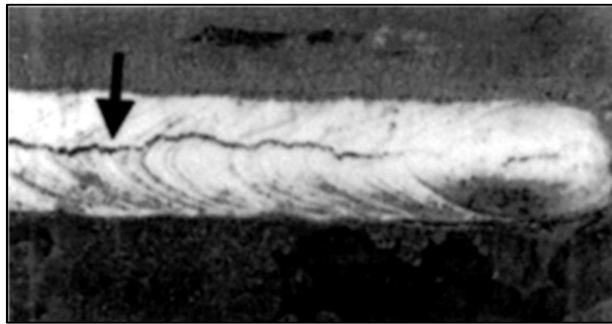


Fig.2.13 Solidification cracking in laser welded sample

c) HAZ liquiation cracking

The low melting point grain boundary films may also be present in the HAZ and may melt and form fine cracks under the influence of the thermal stresses induced during laser welding.



Fig.2.14 HAZ liquiation crack in laser welded sample

d) Stress corrosion cracking

This type of cracking is a failure mechanism which occurs through the combined action of corrosion and tensile stress. Welds which has partial penetration with root cavities are prone to this type of failure and should not be exposed in corrosive medium. Depending upon the corrosive medium this type of cracking can be transgranular or intergranular.

e) Swelling of lap weld

This type of defect may be seen in the thin aluminium sheet where laser welding speed is low and power input is relatively high. It is specially present when the large

amount of material melting of upper sheet respect to the lower plate. This can be prevented by choosing proper heat input and welding speed, improving the thermal conductivity of the sheets and using strong restraint to prevent distortion and deformation of the upper sheet.

f) Inclusions

During the welding process formation of oxides or nitrides are the main reasons for this type of defects. Inclusion leads to solidification cracking and makes the weld weaker. Using proper shielding gases while welding can prevent formation of inclusion. Surface cleaning before the experiment can also play a important role to prevent inclusion.

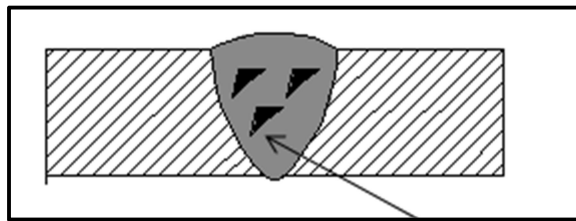


Fig.2.15 Inclusions in laser welded sample

g) Distortion or deformation

Laser welding is a high intensity, high speed welding where the material are subjected to thermal cycles such as melting, evaporation, solidification and cooling, and is inevitably accompanied by volume changes of thermal expansion and contraction all within a very small time. This causes the distortion or deformation, residual stresses in the welded joint. Larger heat inputs, a larger welding molten pools and greater difference between upper and lower bead width are also can be reasons for distortion. Proper fixture, choosing proper speed and power input can minimise the distortion or deformation.

h) Undercut

Along the toe of the weld bead sometime a groove is formed, this is called undercut. Undercutting is generally occurred in a weld where wide bead is made with high power laser or the assist gas pressure is higher or assist gas coming angle is not proper. In laser arc welding due to high arc current it may also occur. Undercut can be prevented using optimised welding condition.

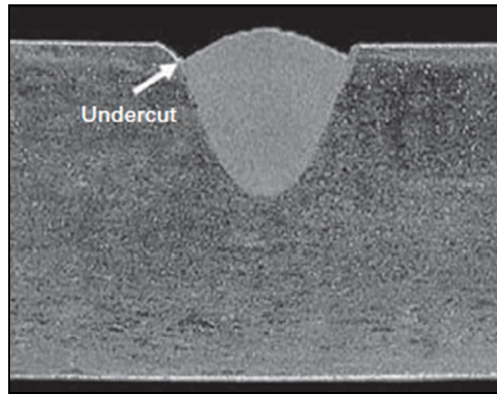


Fig.2.16 Undercut in laser welded sample

i) Underfill

Underfill is the name for a concave surface of a weld bead. It generally occurs due to wide weld gaps in a butt joint with a shortage filler wire, in the case of full penetration weld accompanied with burn through or severe spattering. Underfill can be suppressed by beam scanning, hybrid welding or utilisation of proper filler under proper condition.

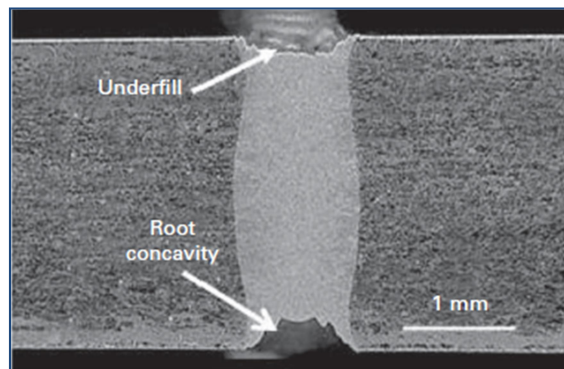


Fig.2.17 Underfill in laser welded sample

j) Humping

Periodical formation of humps of weld metal on the bead surface is called humping. Due to narrow weld bead produced with a focused laser beam during high welding speed it may occur. Humping is formed owing to the backward flow of a melt ejected by plume ejection and the high surface tension of the accumulated melt due to a narrow molten pool width. Humping can be prevented by using defocused beam or avoiding partially penetration of material.

These are some of the main defects which can occur during a laser welding. The optimisation of condition and using assist gas, good fixture can suppress the weld defects, by which more weld strength can be achieved.

2.4 DIFFERENT MODES OF LASER WELDING

Depending on mainly the intensity I , two different welding modes can be obtained viz conduction-mode welding $I < 1 \text{ MW/cm}^2$ (indicatively) and keyhole-mode welding $I > 1 \text{ MW/cm}^2$. Moreover, continuous welds and pulse welds can be distinguished. The pulsed and CW laser welding application generally involves weld penetration in order of 0.010 in and higher.

2.4.1 PULSED MODE OF LASER WELDING

Generally, pulsed laser produces short optical pulses in the form of discrete energy packets transferring small amount of heat on to the part being welded. This laser can produce peak power that is higher than its average peak power. It is used in welding of small parts like battery cases, electronic components, small intricate pieces etc., where the materials cannot be exposed to high heat. For pulsed mode operation, pulsing was carried out by methods like normal pulsing, Q-switching, and mode-locking to achieve pulses in the range of milliseconds to femtoseconds. These short range pulses give instantaneous high peak power for sudden temperature rise and cooling and thereby applied in micro-drilling, nano scale laser processing, and micro-machining of biomaterials and biological components, direct transfer, and micro-printing of functional materials by laser-induced forward transfer (LIFT), thin film deposition, etc

2.4.2 CONTINUOUS MODE OF LASER WELDING

Continuous wave laser emits light continuously till it is stopped. The maximum power cannot be higher than the rated average peak power of the Laser. It is employed when dissimilar metals are to be welded. It can be used in welding of copper to stainless steel or materials with higher thickness etc. Due to the constant output power of the laser, CW mode was mostly used for applications such as surface cladding, glazing, and annealing

Now-a-days, the push towards miniaturization is everywhere. For this conventional welding processes and normal laser beam welding process are not suitable because the excessive heat input leads broad heat affected zone and defects like blow holes in the bead,

distortion etc will occur. Laser micro-welding has been considered as an effective tool for addressing these problems.

It has high-potential advantage in welding of heat sensitive components with precision control of heat input, minimal thermal distortion, small HAZ, good mechanical properties and excellent repeatability. Laser power, scanning velocity, spot diameter and shielding gas are the key parameters to achieve the desired weld. By laser micro welding weld penetration in order of 0.0001in can be achieved.

CHAPTER 3

EXPERIMENTAL INVESTIGATION OF LASER BEAM WELDING OF ALLUMINIUM ALLOY

The weldability of aluminium alloy 2024 is studied in this experimentation. The experiments are designed in such a way that the transition of weld from conduction to keyhole mode is studied. Here aluminium 2024 which consists of 4.4 percent copper is used as the base material. The entire welding process is designed for autogeneous process and hence no filler material is used in the process.

The primary aim of this investigation is to realize satisfactory welds from conduction to keyhole mode in 2 mm thick AA2024 alloy and to obtain the depth of penetration and width of the weld bead along with their mechanical properties. First for narrowing down the laser welding process window screening experiments were carried out as Bead on Plate (BOP) welding and at the same time shielding gas was optimised. After that, with the identified processes window, single pass welding was carried out in pulsed laser mode with Gaussian beam profile. The Gaussian beam is characterised by the attainment of maximum irradiance only at the center of the beam. The Details of each process and characterization are elaborated in the subsequent sub sections.

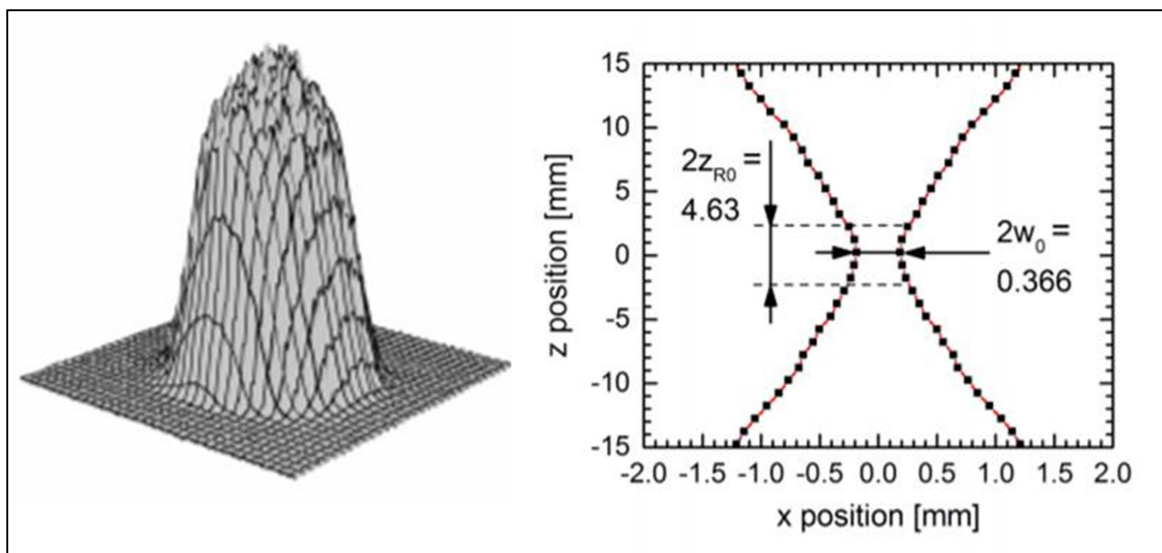


Fig 3.1 Gaussian Beam profile of laser

3.1 MATERIAL COMPOSITION

Aluminium alloy 2024 of 2mm thickness is used as the base material in the welding process. The chemical composition of the material is shown in the table.

Table 3.1 AA 2024, nominal chemical composition (wt.%).

Material	% Min.	% Max.
Cu	3.8	4.9
Mg	1.2	1.8
Mn	0.3	0.9
Fe	-	0.50
Si	-	0.50
Zn	-	0.25
Ti	-	0.15
Cr	-	0.10
Other	-	0.05
Total	-	0.15
Al	Remainder	

3.2 SAMPLE PREPARATION

For the present study, the 2mm thick aluminium alloy were cut into 75mm x 25mm size. The edges of the sample are mechanically filed and sharp edges are removed. The specimen surface is cleaned with a stainless steel wire brush and then with acetone. Once the grease and dirt are removed, the samples are dipped in the 30 percent concentrated Hydrofluoric acid for less than 2 minutes in order to remove the oxide layer. Then the samples are cleaned with water and dried before they are ready for welding.

3.3. EXPERIMENTAL SET UP

3.3.1 PULSED WELDING SYSTEM

All the welding experiments are carried out on the UW YAG 300W pulsed laser welding system. The equipment can handle up to 32 different settings for weld schedules using waveform control. The system incurs minimum energy loss ensures near identical output power for each delivery. The shielding gas output is coaxial with the laser beam output.

Main parts of the welding system are: front cover, up cover, front gate, right gate, left gate, back cover, fibre fixation frame, emergency stop switches and laser switch. The parts are indicated in the figure:3.2. The specifications of the laser welding machine are summerized in Table 3.2.



Fig 3.2 Laser welding machine

Table 3.2 specification of pulsed laser welding machine

Parameter	Value
maximum output power [kW]	300
Mode of operation	Pulsed mode
Maximum single pulse energy [J/Pulse]	100
Pulse width [ms]	30
wavelength [μm]	1.064
laser spot diameter(in focus) [μm]	0.6
irradiance distribution	Gaussian
Cooling mode	Water cooling
Maximum input current [A]	35

Main menu: Fig. 3.3 shows the “main menu” tab of the laser source machine. This enables settings of time, date, no, of good shots, process parameters etc that needed to control the welding machine.

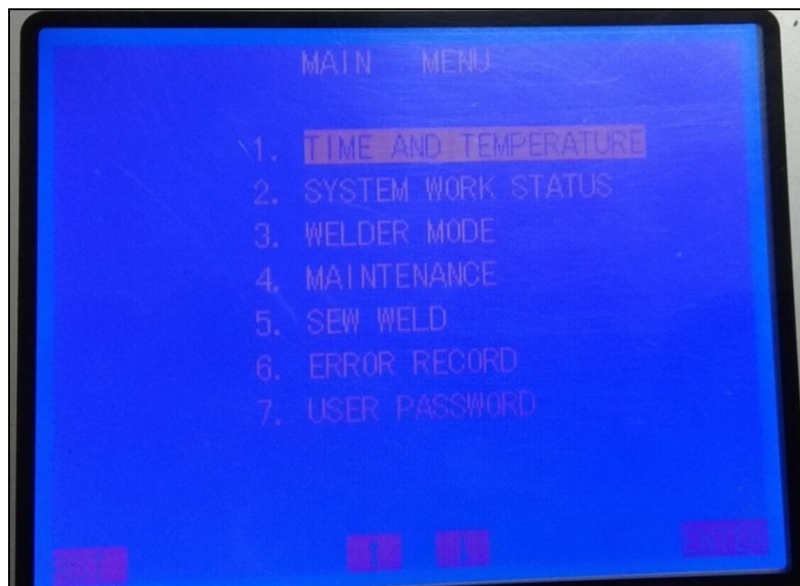


Fig 3.3 main menu of the laser source machine

Welder mode: From this welder mode tab variables of the welding can be changed. In this machine available option to vary are peak power, frequency, pulse width and scanning speed.

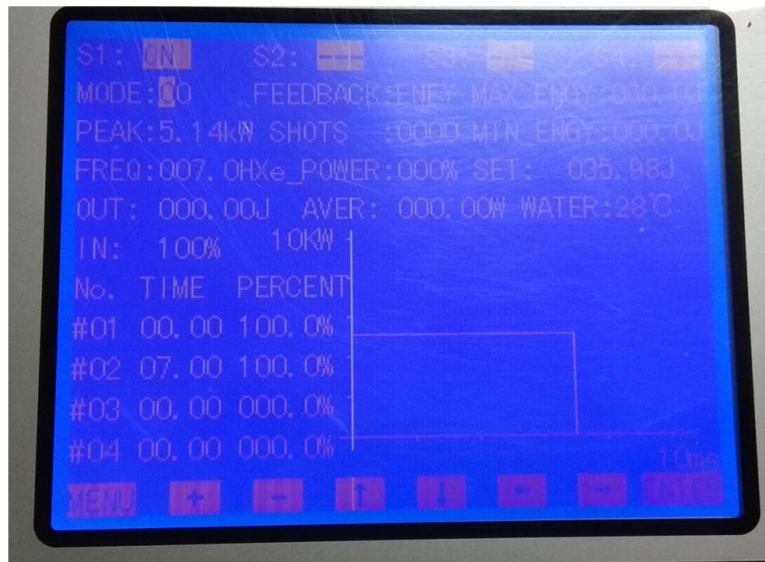


Fig. 3.4 Welder mode of the laser source machine

System work mode: the sub tab shown in Fig. 3.5 indicates the system work mode. During the welding high voltage should be on. Total number shots till the machine shot is also shown.

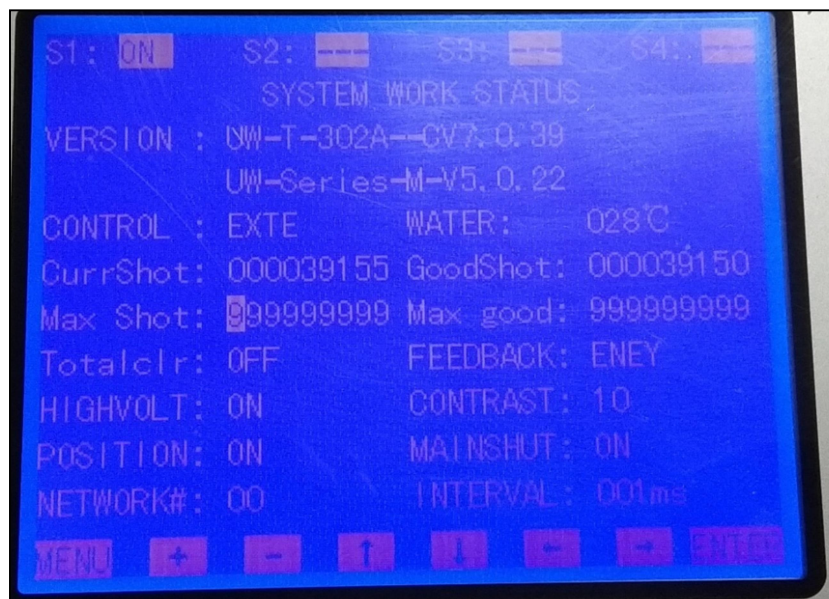


Fig. 3.5 System work status of laser source machine

This welding system is a water cooled system. With the welding system, a chiller unit is also added to maintain the laser system temperature within a safe limit.



Fig. 3.6 Chiller unit

3.3.2. OPTICAL MICROSCOPE

Olympus STM6 optical microscope with 10x zooming is used to take the images of weld and also for weld measurements. With Analysis software data has been collected.



Fig. 3.7 Optical microscope

3.3.3. UNIVERSAL TESTING MACHINE

The Instron 5582 universal testing machine was used to measure the breaking load of the welded specimen. The machine pull the welded sample until it breaks from the joint to measure the tensile strength. By Bluehill software the load elongation curve and data of tensile test has been collected. Maximum tensile load capacity of the machine used for the experiments is 5000N.



Fig. 3.8 Pictorial view of universal testing machine

3.4. EXPERIMENTAL PROCEDURE

3.4.1 WELDING OF LAP JOINTS

In lap welding experimented parameters are chosen such that deep penetration occurs in the metal joint to get the maximum breaking load and variation of breaking load and bond width can be studied during this range. The sample size for the lap joint experiments is 75mm×25mm×2mm. The length of the overlapped portion is 30mm. After sample preparation using proper fixture the welding was done with using argon as assist gas with 3 bar pressure. For the experiment the laser torch has been placed 30 ° angle with the perpendicular axis to focus the lap joint perfectly so that the laser perfectly impinge on the mating line between the two base metals. Same material composition material is used as a backing plate during the welding.

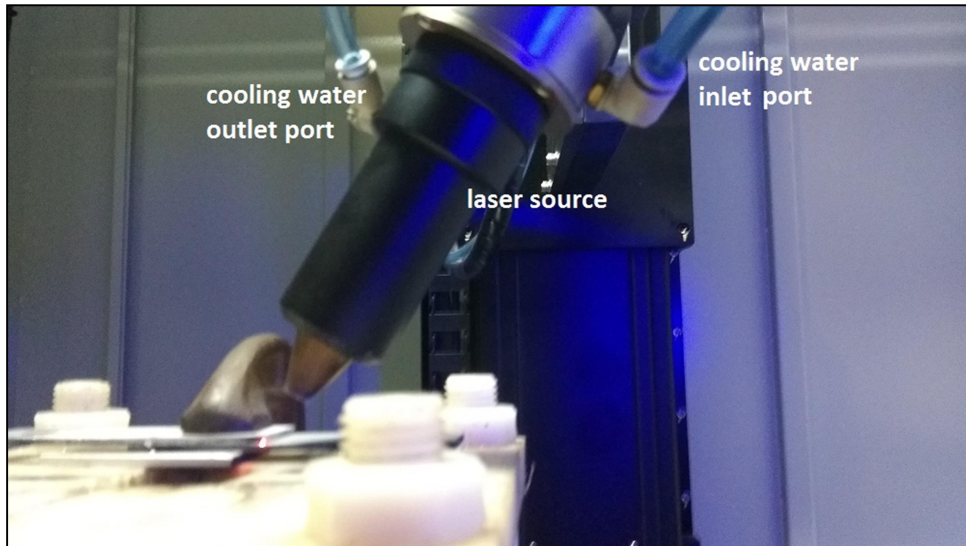


Fig. 3.9 Pictorial view of lap welding of Aluminium 2024 alloy

3.4.2 WELDING OF BUTT JOINTS

The parameters are chosen such that the welding is conducted from the minimum energy needed to weld to the maximum possible output from the machine. The depth of penetration, fusion zone, weld width were calculated along with the tensile strength. The progress in the porosity and cracking levels as the welding progresses from conduction to keyhole are studied. The sample size of the specimen is $75\text{mm}\times 25\text{mm}\times 2\text{mm}$. After the sample preparation for the entire welding process, Argon at 3 bar pressure is used as the shielding gas and same material is used as a backing plate during the welding.

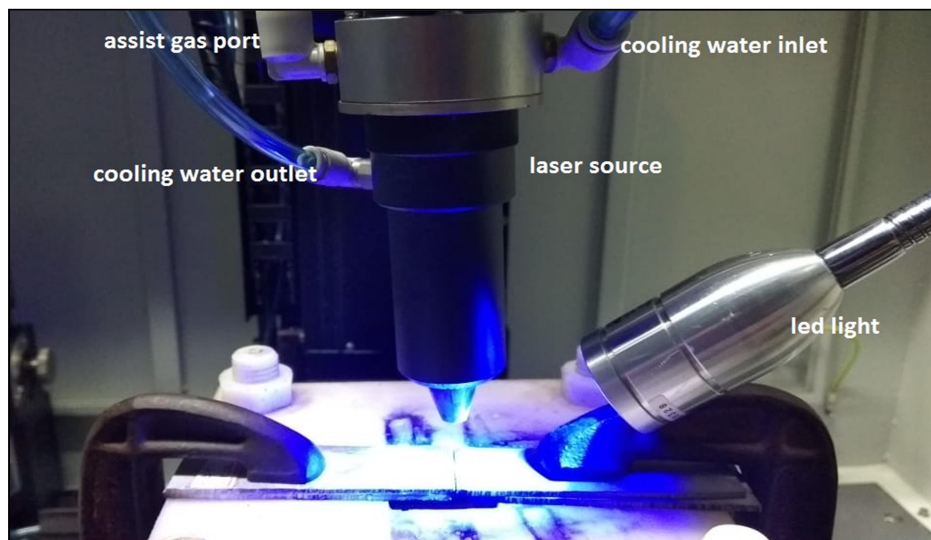


Fig. 3.10 Pictorial view of butt welding set up

3.5 EXPERIMENTAL INVESTIGATION ON LASER BEAM WELDING OF ALUMINIUM ALLOY

3.5.1 EXPERIMENTAL PLAN

The experiments are designed using Taguchi method on Minitab software. The DOE using Taguchi approach can economically satisfy the needs of problem solving and product/process design optimization projects. This technique reduces the time required for experimental investigation. Design of experiments is useful during optimization of product and process design, investigate the effects of multiple factors on the performance etc.

For the experiment to make lap joints L9 process is used to design the experiment i.e. three variables with three levels of data were chosen for the experiments. Varying Peak Power, scanning speed and frequency the experiments were done to see the bond width, theoretical throat length and breaking load of the joint. The levels of parameters were used to design the experiments is tabulated below. The pulse width is fixed at 7 ms for this set of experiment.

Table 3.3 Levels of parameters for lap joint experiment

Parameters	Level 1	Level 2	Level 3
Peak power	4.43	4.79	5.14
Scanning speed	1	1.5	2
Frequency	6	7	8

Using these levels of parameters with Taguchi L9 method 9 experiment sets were designed. The design of experiment is tabulated below.

Table 3.4 Design of experiment of laser lap joint experiment

Sl no.	Peak power (kW)	Scanning Speed (mm/sec)	Frequency (Hz)
1	4.43	1	6
2	4.43	1.5	7
3	4.43	2	8
4	4.79	1	7
5	4.79	1.5	8
6	4.79	2	6
7	5.14	1	8
8	5.14	1.5	6
9	5.14	2	7

For the experiment for butt joint L16 process is used to design the experiment i.e. four variables with four levels of data were chosen to do the experiments. Varying peak power, scanning speed, pulse width and frequency the experiments were done to see weld width and defects presence in the welded joint. The levels of parameters were used to design the experiments is tabulated below.

Table 3.5 Levels of parameters for butt joint experiment

Parameters	Level 1	Level 2	Level 3	Level 4
Peak power	4	4.25	4.5	4.75
Scanning speed	1	1.5	2	2.5
Frequency	6	7	8	9
Pulse width	5	6	7	8

Using this levels of parameters with Taguchi L16 method 16 experiment sets were designed. The design of experiment is tabulated below.

Table 3.6 Design of experiment of laser butt welding

Sl no.	Peak power (kW)	Scanning speed (mm/sec)	Frequency (Hz)	Pulse width (ms)
1	4	1	6	5
2	4	1.5	7	6
3	4	2	8	7
4	4	2.5	9	8
5	4.25	1	7	7
6	4.25	1.5	6	8
7	4.25	2	9	5
8	4.25	2.5	8	6
9	4.5	1	8	8
10	4.5	1.5	9	7
11	4.5	2	6	6
12	4.5	2.5	7	5
13	4.75	1	9	6
14	4.75	1.5	8	5
15	4.75	2	7	8
16	4.75	2.5	6	7

Uses of L9 and L16 process have benefits of conclusions valid over the entire region spanned by the control factors and their settings. These processes make analysis easier and saves large experimental effort.

3.5.2 ANALYSIS OF EXPERIMENTAL RESULTS OF LAP JOINT

3.5.2.1 RESULTS

Using the L9 methods experiment sets were formed for laser lap welding. The experiments were done and the responses i.e. breaking load was measured using universal testing machine and using optical microscope bond width and theoretical throat length were measured. Experiment results are tabulated below.

Table 3.7 Results of lap welding experiments

Sl no.	Peak power P (kW)	Scanning speed V (mm/sec)	Frequency f (Hz)	Breaking load (N)	Bond width (μm)	Throat length (μm)
1	4.43	1	6	188	398.81	340.72
2	4.43	1.5	7	520	434.79	350.95
3	4.43	2	8	727	474.37	427.40
4	4.79	1	7	1233	713.01	731.53
5	4.79	1.5	8	594	954.76	983.94
6	4.79	2	6	445	496.56	369.99
7	5.14	1	8	230	854.45	772.51
8	5.14	1.5	6	330	507.23	385.39
9	5.14	2	7	712	552.69	417.32

Images of lap welded joints after tensile strength testing are given below. These images are taken with 10x zooming in optical microscope.

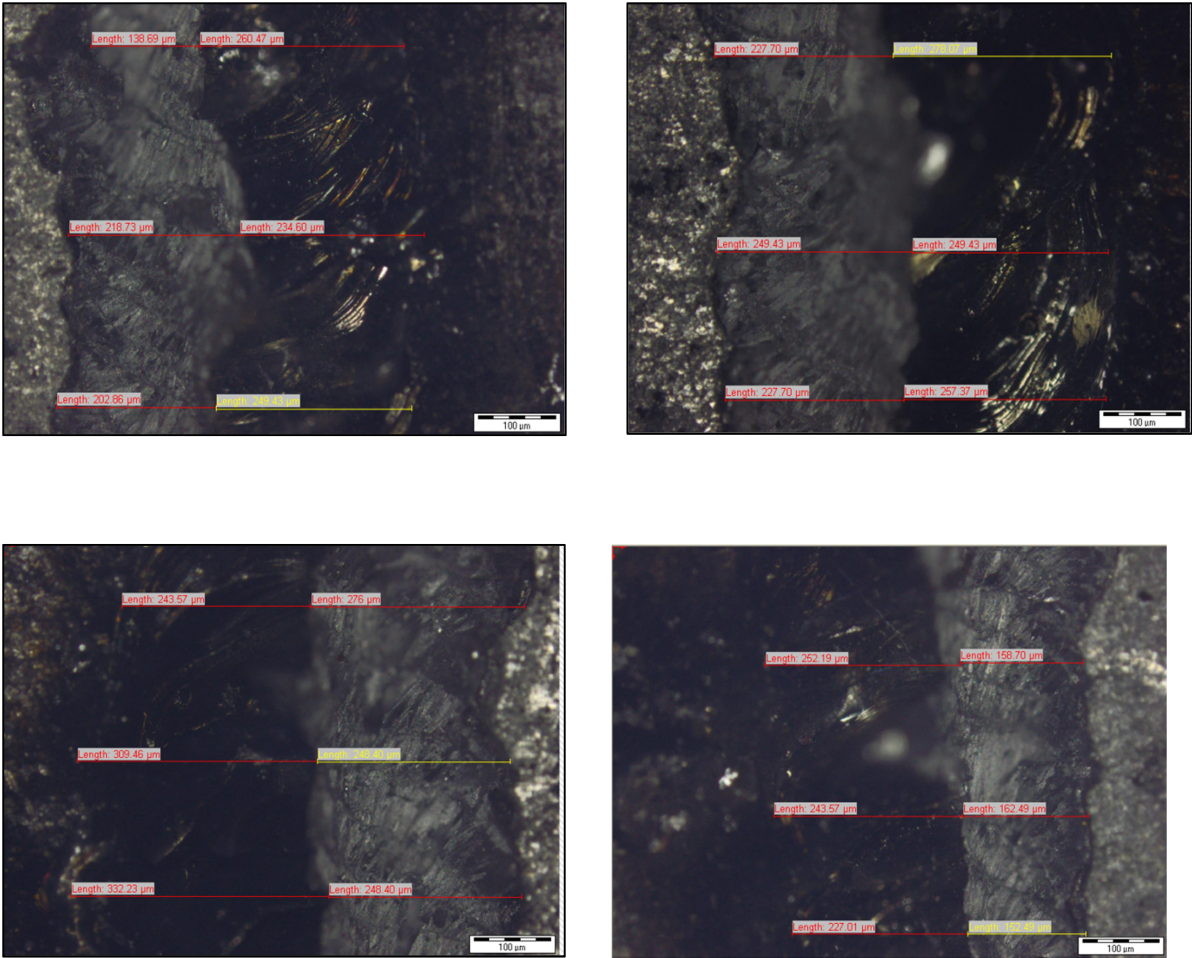


Fig. 3.11 Laser welded lap joint

3.5.2.2 EFFECT OF PROCESS PARAMETER ON BOND WIDTH

After the completion of the experiments bond width was measured using optical microscope with 10x zooming. Taking that data several types of graphs are plotted for analysis.

a) Analysis on main effect plots of bond width

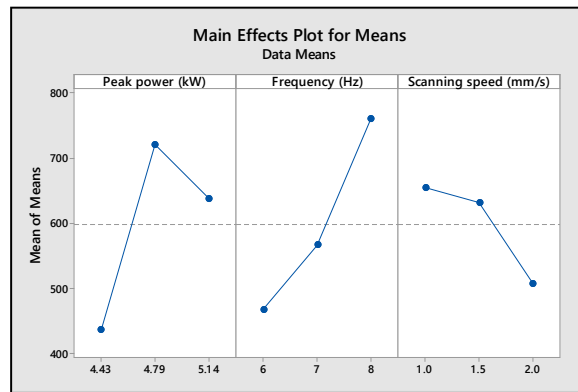


Fig. 3.12 Main effect plots for bond width

From the above main effect plot of bond width it is observed that with increase of peak power will increase the bond width upto a certain limit because in this range more energy involved with more power but after certain a certain limit it tends to decrease because more power will fully penetrates the plate which is the loss of energy and energy accumulation becomes lower. Bond width increases with frequency because more frequency will cause more average power and that will accumulate more energy. For increasing scanning speed bond width will decrease because when laser move faster less time to deliver energy to the material causes lesser bond width. For maximum bond width the parameters combination will be – Peak power 4.79 kW, scanning speed 1mm/sec and frequency 8Hz

b) Analysis on surface plots of bond width

The regression equation of bondwidth –

$$\text{Bond width} = -27709 + 13248 P - 411.7 V - 1182 f - 1452 P*P - 261.9 V*V + 67.28 f*f + 225.7 P*V + 84.96 P*f$$

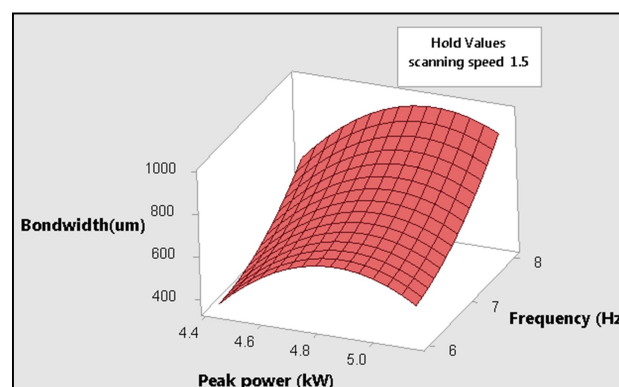


Fig. 3.13 Bond with vs peak power,frequency

The above figure is bond width vs peak power and frequency graph keeping scanning speed constant at 1.5 mm/sec. it is observed from the above graph that for a fixed peak power bond width increases when frequency increases because as frequency increases average power is also increases and laser impact on the material more rapidly. For a particular frequency when peak power increases bond width also increases upto a limit then it decreases with increase of peak power. Because when peak power increases average power also increases, that will increase the bond width due to more power. But after a certain limit if the peak power

increases it has more impinge power and the laser penetrates the 2mm thickness aluminium, thus due to loss of energy the bond width tends to reduce.

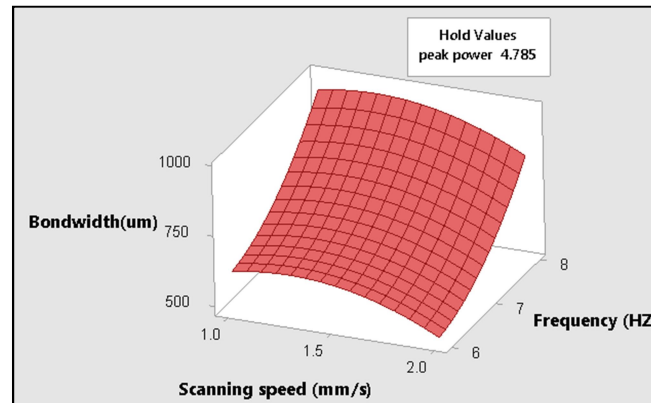


Fig. 3.14 Bond width vs scanning speed, frequency

the above figure is bond width vs scanning speed and frequency graph, where peak power is constant at 4.785 kW. From the figure it is observed that for a particular scanning speed if frequency increases bond width increases because when peak power is constant for more frequency, more average power will produce which makes the bond width larger. And for a particular frequency, bond width is decreasing when scanning speed is increasing because when scanning speed increases heat accumulation in a point decreases, so the bond width decreases.

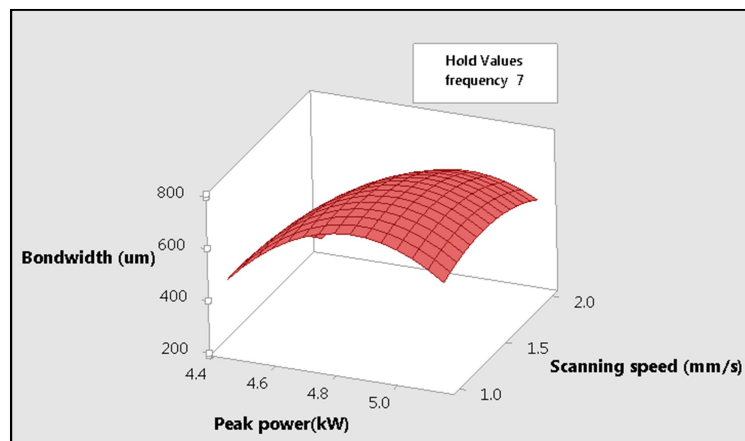


Fig. 3.15 Bond width vs peak power, scanning speed

The above graph is bond width vs peak power, scanning speed graph at fixed frequency 7 Hz. From the graph it is observed that at a fixed scanning speed bond width increases with peak power first then after a certain point it tends to decrease. This is because more peak power will increase the average power and energy accumulation in welding zone, but after a certain point due to excessive peak power laser penetrates the plates fully and passes through the

plate, this decreases the energy accumulation, so the bond width tends to decrease. For a low peak power if scanning speed increases bond width decreases as the laser moving faster the energy accumulation in a weld point becomes lower, makes the smaller bandwidth.

c) analysis on contour plots of bond width

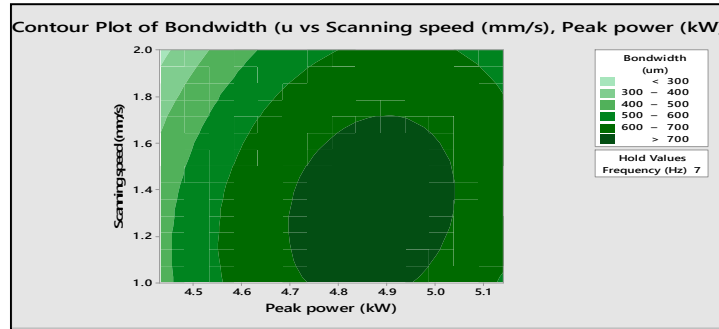


Fig. 3.16 Contour plot of bond width vs peak power, scanning speed

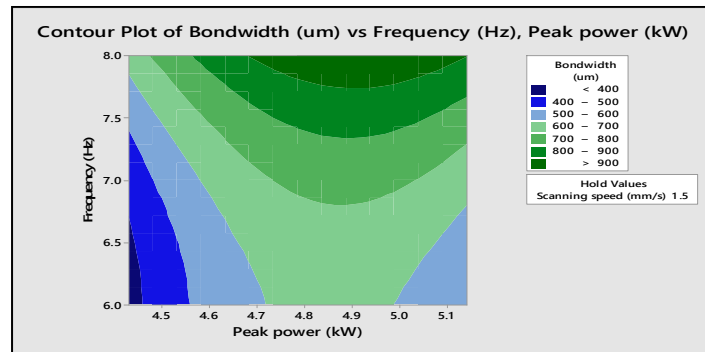


Fig. 3.17 Contour plot of bond width vs peak power, frequency

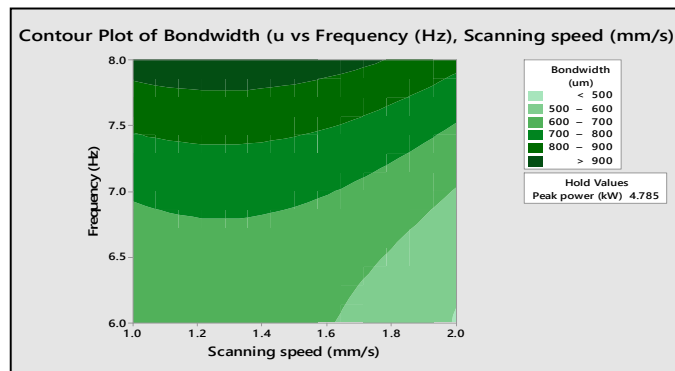


Fig. 3.18 Contour plot of bond width vs frequency, scanning speed

The above figures are contour plots of bond width vs. combination of experiment parameters (peak power, scanning speed and power, frequency and frequency, scanning speed). From the contour graph for a chosen bond width corresponding range parameters can be calculated.

3.5.2.3 EFFECT OF PROCESS PARAMETRS ON BRAEKING LOAD

After completion of experiment, the tensile test of each samples were measured using UTM with maximum load capacity of 5 kN. The data were recorded and using the data graphs are plotted using Minitab software for analysis.

a) Analysis on main effect plots of breaking load

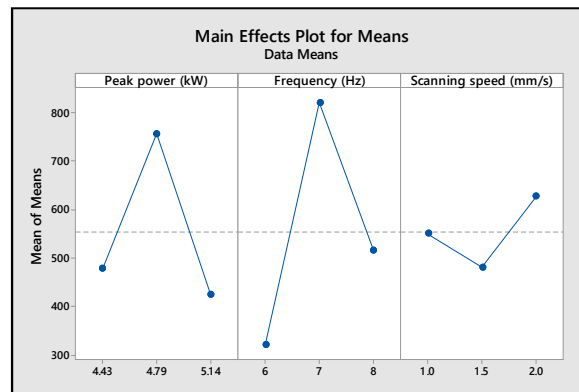


Fig. 3.19 Main effect plots for breaking load

From the above S/N ratio curves of breaking load it is observed that with increase of peak power and frequency breaking load of the joint also increases to a certain limit, then it is decreasing and with Increase of scanning speed breaking load first decreases then it increases after certain limit. Increase of power and frequency increases the energy accumulation on a point of weld, which increases the weld strength but after certain limit if more energy applied the material starts evaporate, that makes a weld weak. And in some ranges for scanning speed when scanning speed increases the breaking load decreases due to low energy consumption for fast movement of laser, and for some range with increase of scanning speed breaking increases if in the earlier scanning speed makes material evaporation, increasing speed will give stronger joint. For maximum breaking load the combination of parameters will be –

Peak power 4.79 kW, frequency 7, scanning speed 2mm/sec.

b) Analysis on surface plots of breaking load

The regression equation for breaking load is

$$\text{Breaking load} = -100293 + 29581 P - 6555 V + 10030 f - 2433 P*P + 1156 V*V - 351.6 f*f + 583.7 PV - 1036 P*f$$

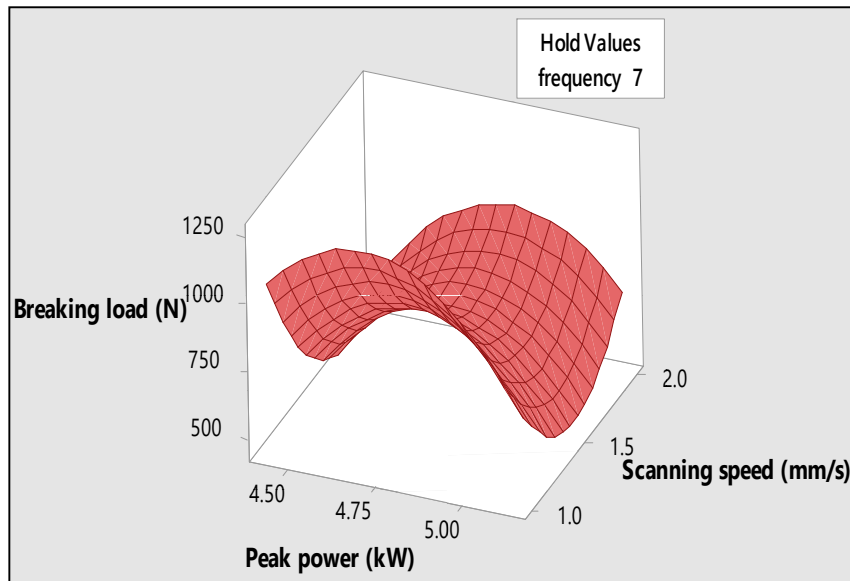


Fig. 3.20 Breaking load vs peak power, scanning speed

In the above figure change of breaking load with peak power and scanning speed is shown when frequency is constant. It is observed that for a fixed scanning speed breaking load increases with peak power upto a certain limit, then tends to decrease. Because when the peak power increases depth of penetration increases as more energy is involved, but after a certain limit, the energy accumulation become excessive which results vaporization of melting zone metal and undercut, this makes the weld weaker. And for a lower fixed peak power at higher scanning speed breaking load is decreasing as the laser moves fast makes the low energy accumulation.

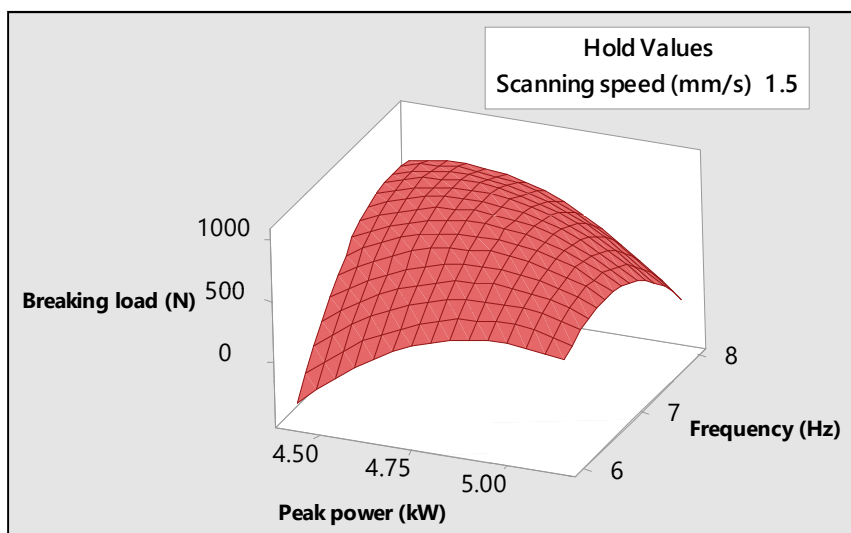


Fig. 3.21: Breaking load vs peak power, frequency

In the above graph change of breaking load with peak power and frequency is shown at fixed scanning speed at 1.5 mm/s. It is observed from the graph that for a lower peak power breaking load is increasing with frequency due to more average energy causing more energy involvement. But at a higher fixed peak power, after increasing to a certain limit breaking load tends to decrease with increase of frequency. Because at the maximum breaking point corresponding frequency gives full penetration, more frequency causes the laser penetrate completely and that makes energy wastage, and also evaporation of weld metal and undercutting. That makes the breaking load lower. At lower frequency when peak power increases breaking load increases because more frequency accumulate more energy to the weld. But at higher frequency breaking load decreases when peak power increases. Because as it already full penetrating at the lower frequency, more frequency results evaporation of weld metal, with makes weld weaker.

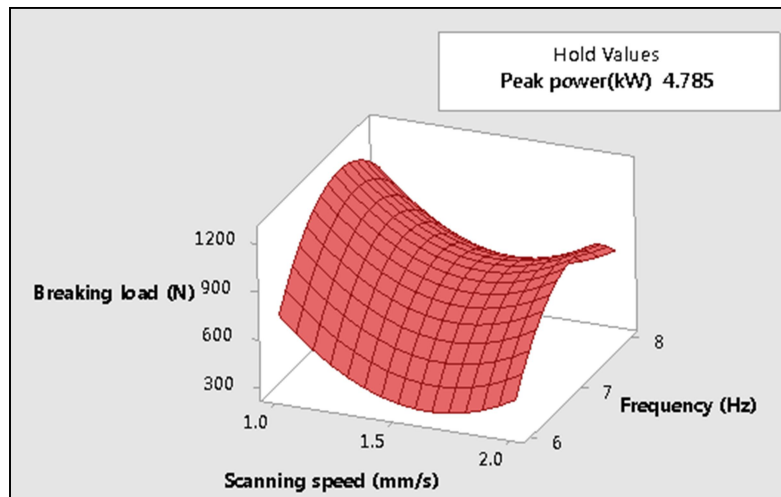


Fig. 3.22 Breaking load vs scanning speed, frequency

In the above graph change of breaking load with scanning speed and frequency is shown at fixed peak power 4.785 kW. It is observed from the graph for a fixed frequency if scanning speed decreases breaking load will decrease due to less energy absorbed by the material and for a for a fixed scanning speed breaking load is increases with frequency upto a certain limit then decreases. Because more frequency means more energy and that makes joint stronger but after a certain limit more energy will start to evaporate the material from joint, it makes the joint weaker.

c) Analysis on contour plots of breaking load

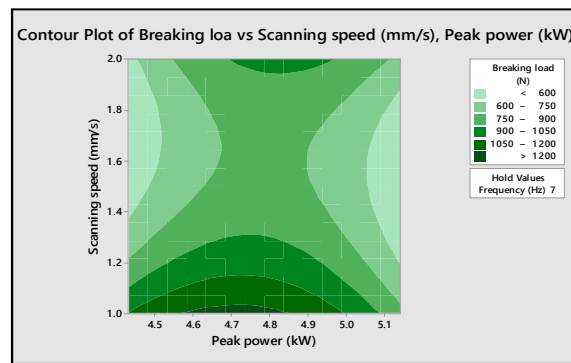


Fig. 3.23 Contour plot of breaking load vs peak power, scanning speed

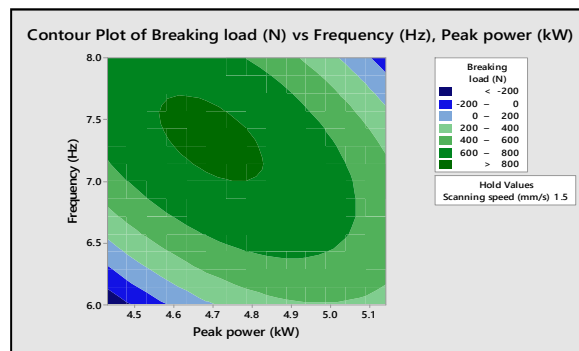


Fig. 3.24 Contour plot of breaking load vs peak power, frequency

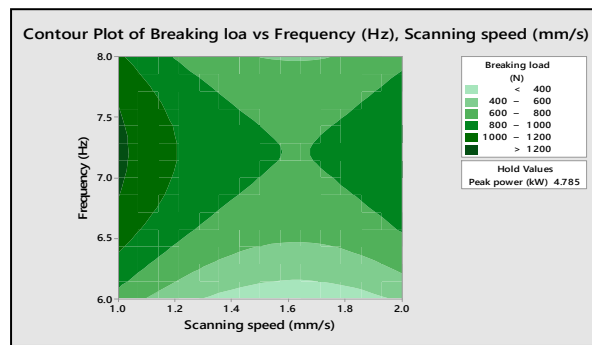


Fig. 3.25 Contour plot of breaking load vs frequency, scanning speed

The above figures are contour plots of breaking load vs. combination of experiment parameters (peak power, scanning speed and power, frequency and frequency, scanning speed). From the contour graph for a chosen breaking load corresponding range parameters can be calculated.

3.5.2.4 EFFECT OF PROCESS PARAMETER ON THROAT LENGTH

After the completion of the experiments throat length was measured using optical microscope with 10x zooming. Taking that data several types of graphs are plotted for analysis.

a) Analysis on main effect plots of throat length

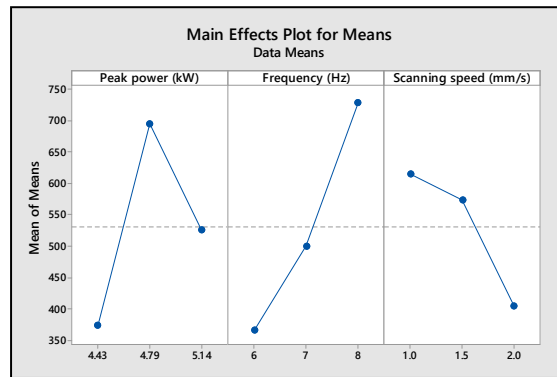


Fig. 3.26 Main effect plots for throat length

From the above S-N ratio curves of throat length it is observed that with increase of peak power will increase the theoretical throat length upto a certain limit because in this range more energy involved with more power but after certain a certain limit it tends to decrease because more power will fully penetrates the plate which is the loss of energy and energy accumulation becomes lower. Throat length increases with frequency because more frequency will cause more average power and that will accumulate more energy. For increasing scanning speed theoretical throat length will decrease because when laser move faster less time to deliver energy to the material causes lesser throat length. For maximum throat length the parameters combination will be –

Peak power 4.79 kW, scanning speed 1mm/sec and frequency 8Hz

b) Analysis on surface plots of throat length

The regression equation of theoretical throat length is

$$\text{Throat length} = -40597 + 18472 \times P - 1820 \times V - 766.2 \times f - 1945 \times P \times P - 218.9 \times V \times V + 87.84 \times f \times f + 469.9 \times P \times V - 50.21 \times P \times f$$

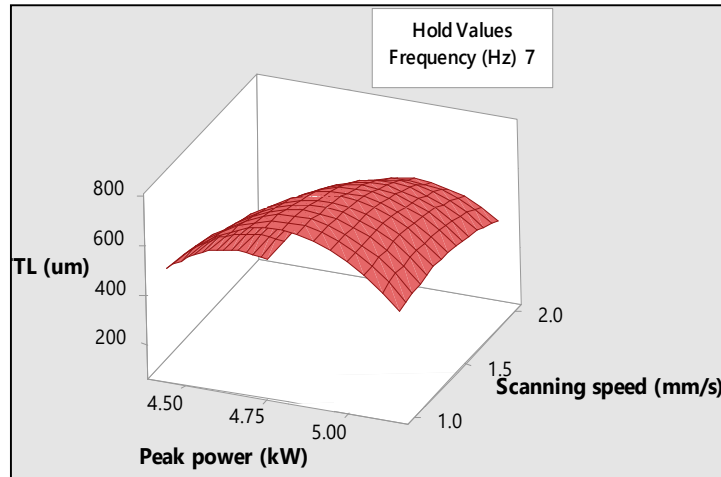


Fig. 3.27 Throat length vs peak power, scanning speed

The above graph is throat length (TL) vs peak power, scanning speed graph at fixed frequency 7 Hz. From the graph it is observed that at a fixed scanning speed theoretical throat length increases with peak power first then after a certain point it tends to decrease. This is because more peak power will increase the average power and energy accumulation in welding zone, but after a certain point due to excessive peak power laser penetrates the plates fully and passes through the plate, this decreases the energy accumulation, so the theoretical throat length tends to decrease. For a low peak power if scanning speed increases theoretical throat length decreases as the laser moving faster the energy accumulation in a weld point becomes lower, makes the smaller theoretical throat length.

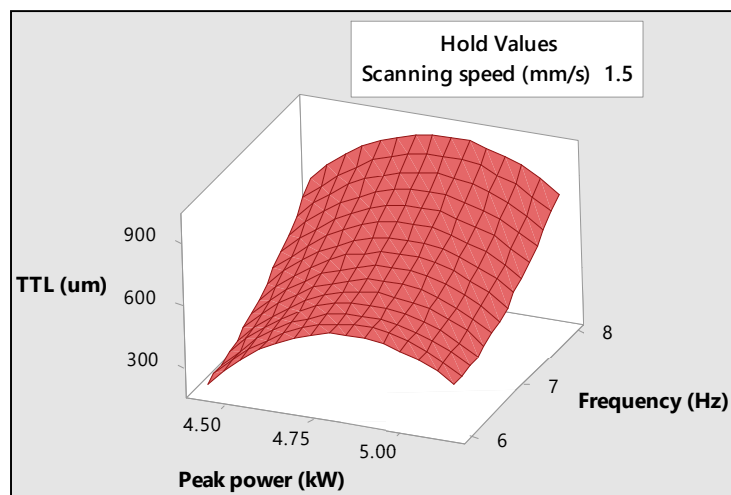


Fig. 3.28 Throat length vs peak power, frequency

The above figure is throat length vs peak power and frequency graph keeping scanning speed constant at 1.5 mm/sec. it is observed from the above graph that for a fixed peak power theoretical throat length increases when frequency increases because as frequency increases

average power is also increases and laser impact on the material more rapidly. For a particular frequency when peak power increases throat length also increases upto a limit then it decreases with increase of peak power. Because when peak power increases average power also increases, that will increase the theoretical throat length due to more power. But after a certain limit if the peak power increases it has more impinge power and the laser penetrates the 2mm thickness aluminium, thus due to loss of energy the throat length reduced.

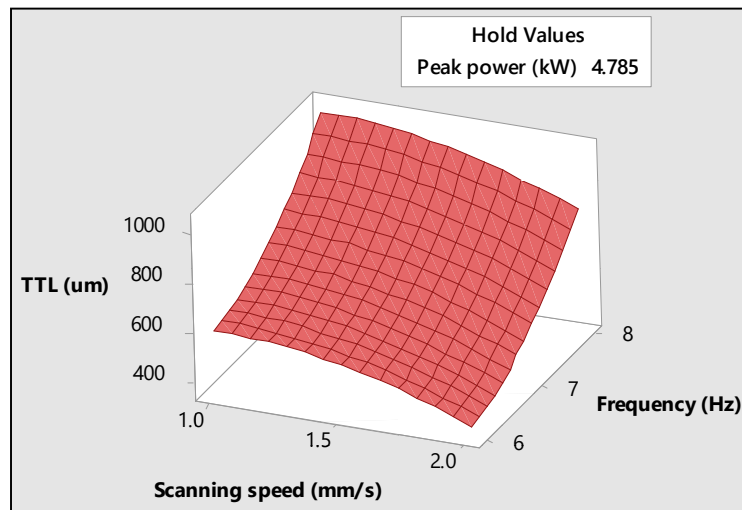


Fig. 3.29 Theoretical; throat length vs scanning speed, frequency

the above figure is throat length vs scanning speed and frequency graph, where peak power is constant at 4.785 kW. From the figure it is observed that for a particular scanning speed if frequency increases throat length increases because when peak power is constant for more frequency, more average power will produce which makes the throat length larger. And for a particular frequency, throat length is decreasing when scanning speed is increasing because when scanning speed increases heat accumulation in a point decreases, so the throat length decreases.

c) Contour plot analysis of throat length

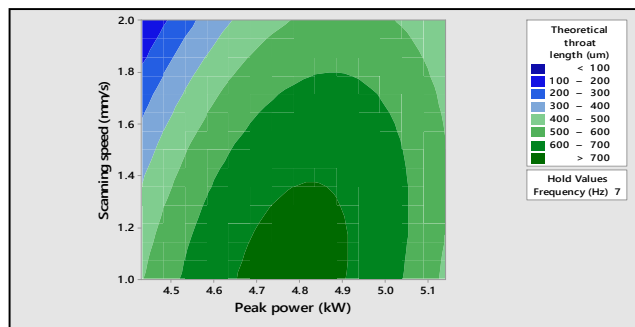


Fig. 3.30 Contour plot of throat length vs peak power, scanning speed

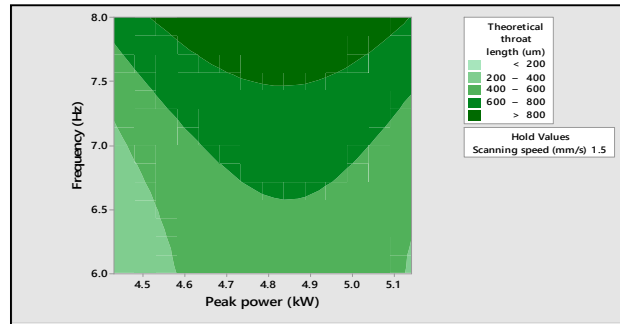


Fig. 3.31 Contour plot of throat length vs peak power, frequency

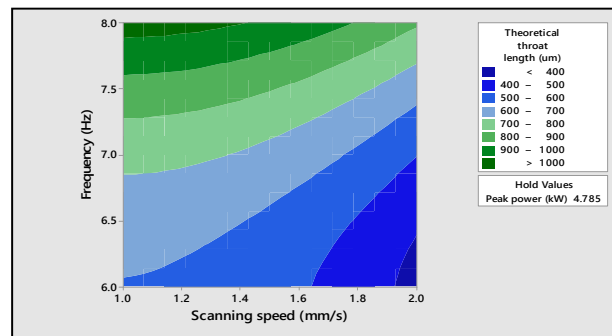


Fig. 3.32 Contour plot of throat length vs frequency, scanning speed

The above figures are contour plots of throat length vs. combination of experiment parameters (peak power, scanning speed and power, frequency and frequency, scanning speed). From the contour graph for a chosen theoretical throat length corresponding range parameters can be calculated.

3.5.3 ANALYSIS OF EXPERIMENTAL RESULTS OF BUTT JOINT

3.5.3.1 RESULTS

Using the L16 method laser butt welding experiments were done. And using the microscope the response has been measured. The sets of experiments with corresponding response are tabulated in table 3.8

Table 3.8 Results of butt welding experiments

Sl no.	Peak power P (kW)	Scanning speed V (mm/sec)	Frequency f (Hz)	Pulse width PW (ms)	Welding width (μm)
1	4	1	6	5	1357.46
2	4	1.5	7	6	1616.9
3	4	2	8	7	1592.98
4	4	2.5	9	8	1827.12
5	4.25	1	7	7	1877.65
6	4.25	1.5	6	8	1909.33
7	4.25	2	9	5	1373.79
8	4.25	2.5	8	6	1394.26
9	4.5	1	8	8	2043.33
10	4.5	1.5	9	7	1752.95
11	4.5	2	6	6	1560.2
12	4.5	2.5	7	5	1555.72
13	4.75	1	9	6	1661.98
14	4.75	1.5	8	5	1513.67
15	4.75	2	7	8	1547.9
16	4.75	2.5	6	7	1701.08

The images of butt welded joints are given below. The images were taken with 10x zooming in optical microscope.

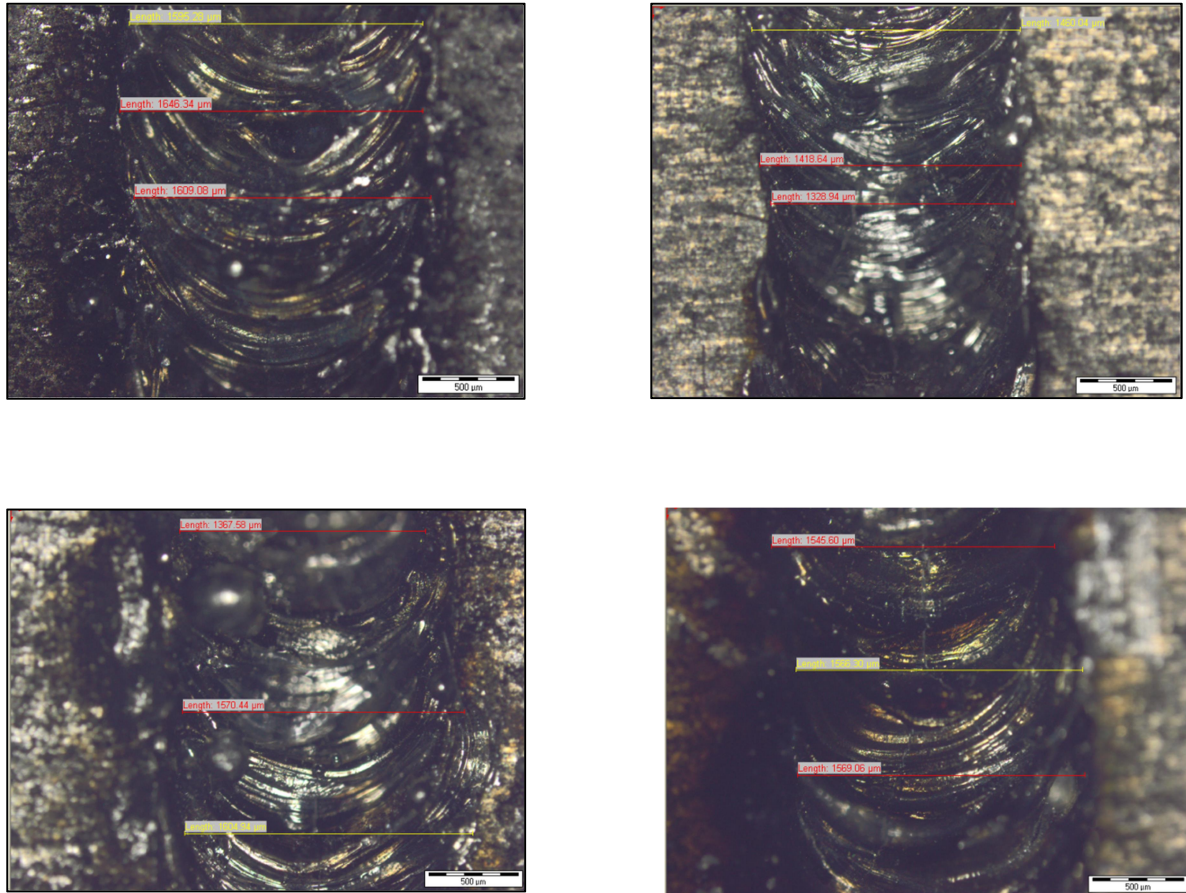


Fig. 3.33 Butt welded joint

3.5.3.2 EFFECT OF PROCESS PARAMETERS ON WELD WIDTH

a) Mean effect plot analysis for weld width



Fig. 3.34: main effects plot for welding width

In the above figure main effects for welding width is shown. From the graph it is observed that when peak power increases weld width also increases to a certain limit(4.5 kW) because if peak power increases average power and energy accumulation on the weld also increases , that makes weld width larger but after that due to high peak power the laser beam complete penetrates and laser beam passing through the plate, that causes loss of energy, which makes weld width lower. With increase of scanning speed weld width tends to decrease due to fast movement of laser causing less energy transfer for a weld point. If frequency increases weld width also increases because more frequency causes more repetition of lasing action i.e. more energy density on weld. When pulse width increases weld width also increases because pulse width increases the average power of the laser also increases. From the graph it can conclude that for getting lowest weld width the value of the parameter should be

Peak power = 4.0 kW

Scanning speed = 2 mm/s

Frequency = 6 Hz

Pulse width = 5 mS

b) Pareto Chart analysis for weld width

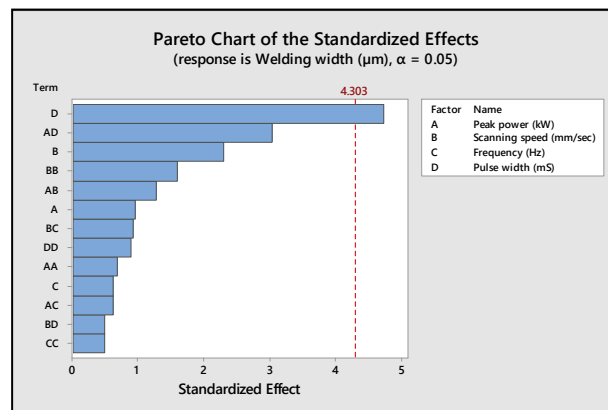


Fig. 3.35 Pareto chart of the standardized effects of welding width

From Pareto chart analysis of weld width it can be concluded that among the process parameters pulse width has the highest effect on the weld width.

c) Surface plot analysis for weld width:

Regression equation of weld width

$$\begin{aligned} \text{Welding width } (\mu\text{m}) = & -51057 + 21778 \times P - 1261 \times V + 1860 \times f + 22 \times P \times PW - \\ & 2318 \times P \times P + 137.7 V \times V - 52 f \times f + 89 PW \times PW + 452 P \times V - 95 P \times f - 323 P \times PW - \\ & 365 V \times f + 209 V \times PW \end{aligned}$$

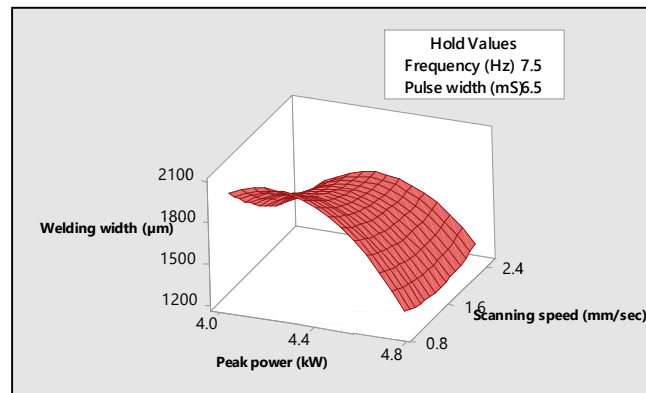


Fig. 3.36 Welding width vs peak power, scanning speed

In the above figure variation of welding width with peak power and scanning speed is shown at fixed frequency at 7.5 Hz and pulse width 6.5 mS. It is observed from the figure that for a fixed scanning speed weld width increases when peak power increases for a certain limit then it tends to decrease. Because until the full penetration was done energy accumulation increases with peak power but after that limit laser penetrate the full width this causes loss of energy density results lowering the weld width. For a lower fixed peak power when scanning speed increases weld width decreases. When velocity of the laser increased the lasing action time is reduced, that reduces the heat accumulation at the weld joint results reduction in weld width.

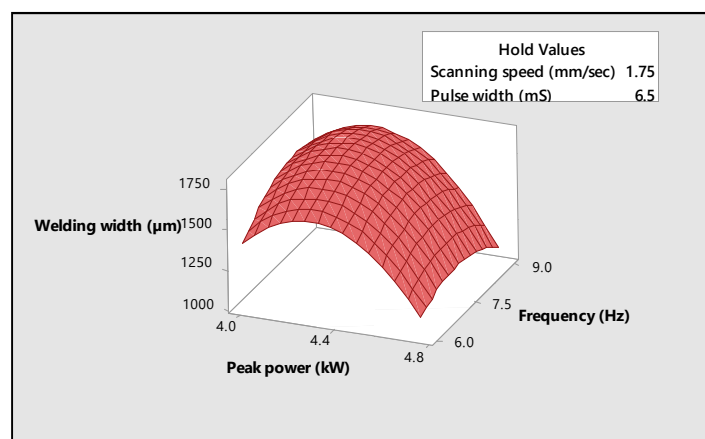


Fig. 3.37 Welding width vs peak power, frequency

In the above figure variation of welding width with peak power and frequency is shown at fixed scanning speed at 1.75 mm/sec and pulse width 6.5 mS. It is observed from the figure

that for a fixed frequency weld width increases when peak power increases for a certain limit then it tends to decrease. Because until the full penetration was done energy accumulation increases with peak power but after that limit laser penetrate the full width of the plate, this causes loss of energy density results lowering the weld width. For a fixed peak power, weld width first increases to a certain limit then tends to decrease with increase of frequency. The frequency directly proportional to average power, increase of frequency results increase of average power, so weld width starts to increase, but after that saturation pint due to loss of energy it decreases.

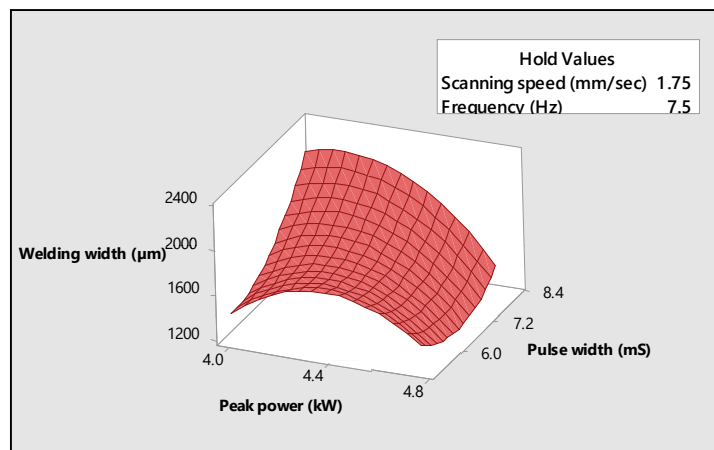


Fig. 3.38 Welding width vs. welding width, pulse width

In the above figure variation of welding width with peak power and pulse width is shown at fixed scanning speed at 1.75 mm/sec and frequency 7.5 Hz. From the figure it is evident that for a weld width increases when pulse width increases. Pulse width directly proportional to the average power which increases the energy density at the weld results increase of weld width.

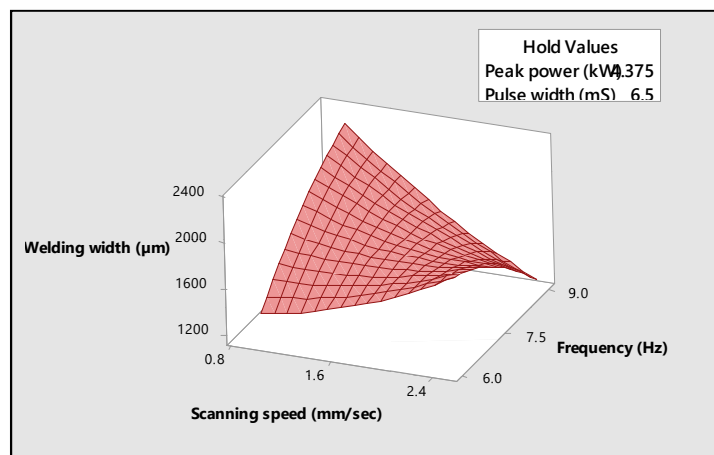


Fig. 3.39 Welding width vs. scanning speed, frequency

In the above figure, variation of weld width with scanning speed and frequency at a peak power of 4.375 kW and a pulse width of 6.5ms is depicted. For a higher frequency, increasing scanning speed has decreased the weld width. This is because higher scanning speed will decrease the time of energy transfer to a weld point, that reduces the weld width. For a lower fixed scanning speed, weld width increases with frequency due to more average power creation.

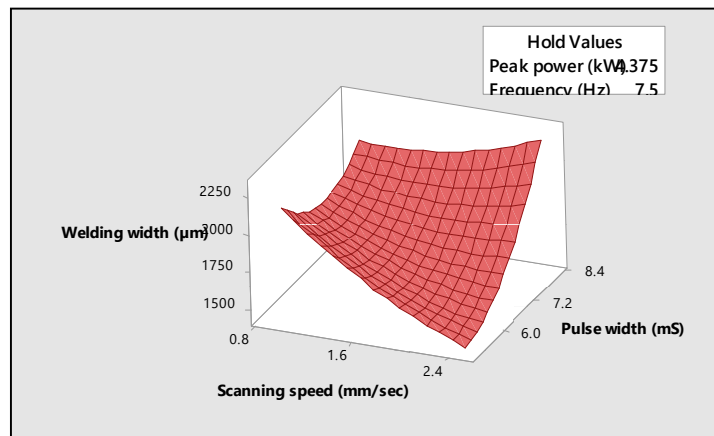


Fig. 3.40 Welding width vs. scanning speed, pulse width

The above figure shows the variation of weld width with scanning speed and pulse width when peak value is fixed at 4.375 kW and frequency 7.5 Hz. For a fixed scanning speed increase of pulse width results increase of weld width due to more average power and more pulse on time heat transfer time will be larger, that increases the weld width. For a lower pulse width, if scanning speed increases welding width will decrease, because laser gets lesser time to transfer heat to a point.

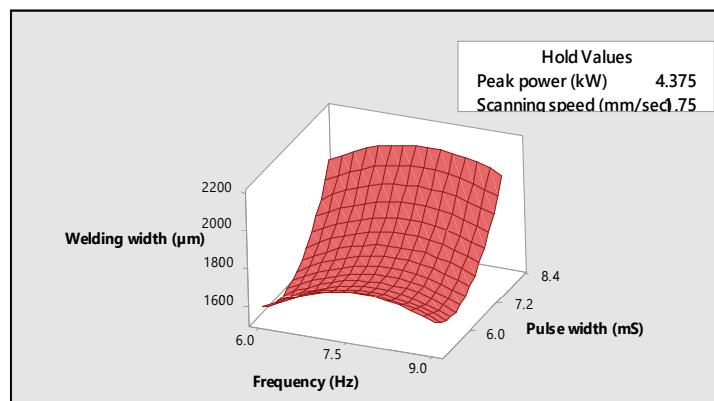


Fig. 3.41 Welding width vs. frequency, pulse width

The above figure signifies the change of weld width with respect to frequency and pulse width at fixed peak power at 4.375 kW and scanning speed at 7.5mm/sec. It is observed from

the graph that for a fixed frequency if pulse width increases weld width increases. Pulse width directly proportional to the average power which increases the energy density at the weld results increase of weld width. For a fixed pulse width when frequency increases weld width increases upto a limit then decreases. For a fixed pulse width weld width first increases to a certain limit then tends to decrease with increase of frequency. The frequency directly proportional to average power, increase of frequency results increase of average power, so weld width starts to increase, but after that saturation point due to loss of energy it decreases.

d) Contour plots analysis of welding width

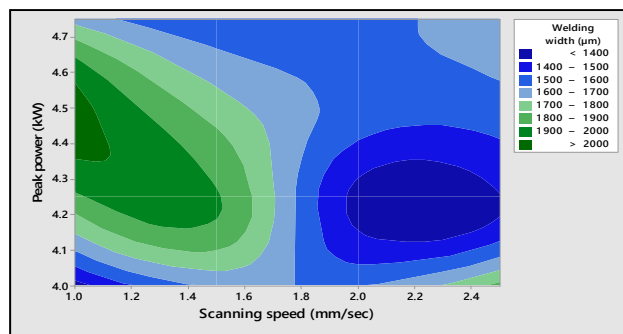


Fig. 3.42 Contour plot of welding width vs peak power, scanning speed

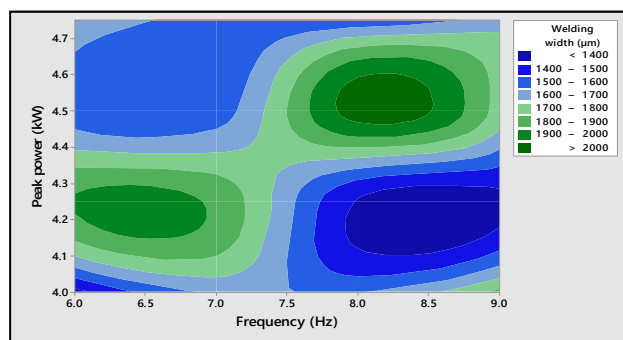


Fig. 3.43 Contour plot of welding width vs peak power, frequency

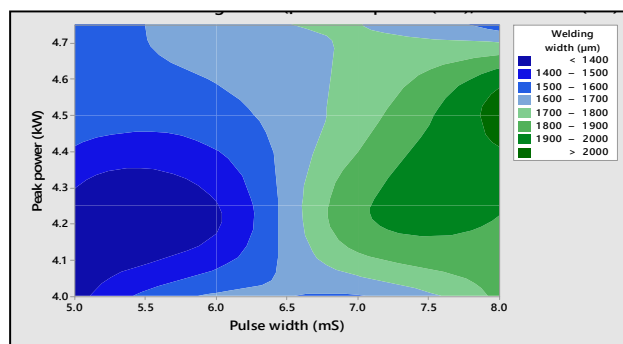


Fig. 3.44 Contour plot of welding width vs peak power, pulse width

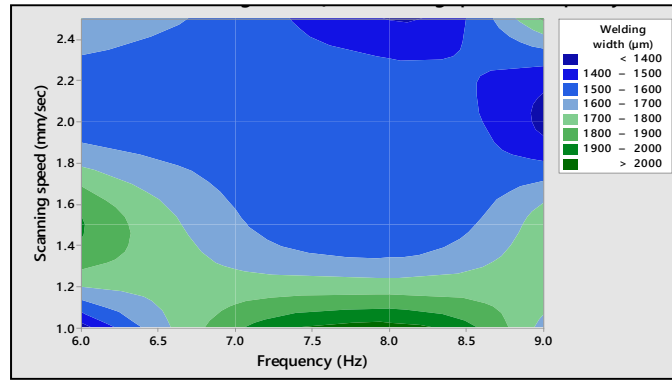


Fig. 3.45 Contour plot of welding width vs scanning speed, frequency

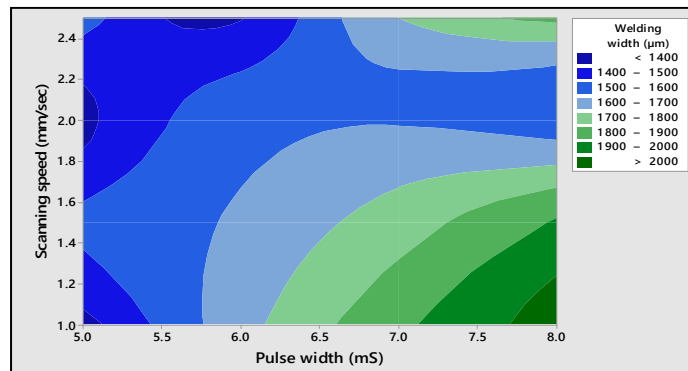


Fig. 3.46 Contour plot of welding width vs scanning speed, pulse width

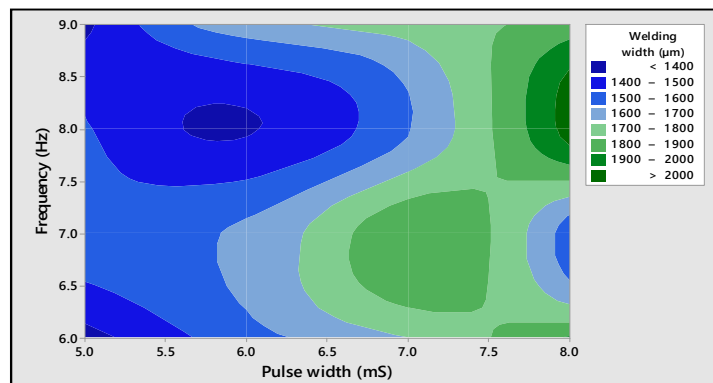


Fig. 3.47 Contour plot of welding width vs frequency, pulse width

The above figures are contour plots of welding width vs. combination of different experimental parameters (peak power, scanning speed, frequency and pulse width). From the contour graph for a chosen breaking load corresponding range parameters can be calculated

3.5.3.3 ANALYSIS OF CRACKS AND PORES

Aluminium alloys are very prone to pores and cracks. Trends on pores and cracks has been analysed in the laser welded butt joint by observation through 20x zooming by optical microscope. The images of cracks and pores for different samples are given below.

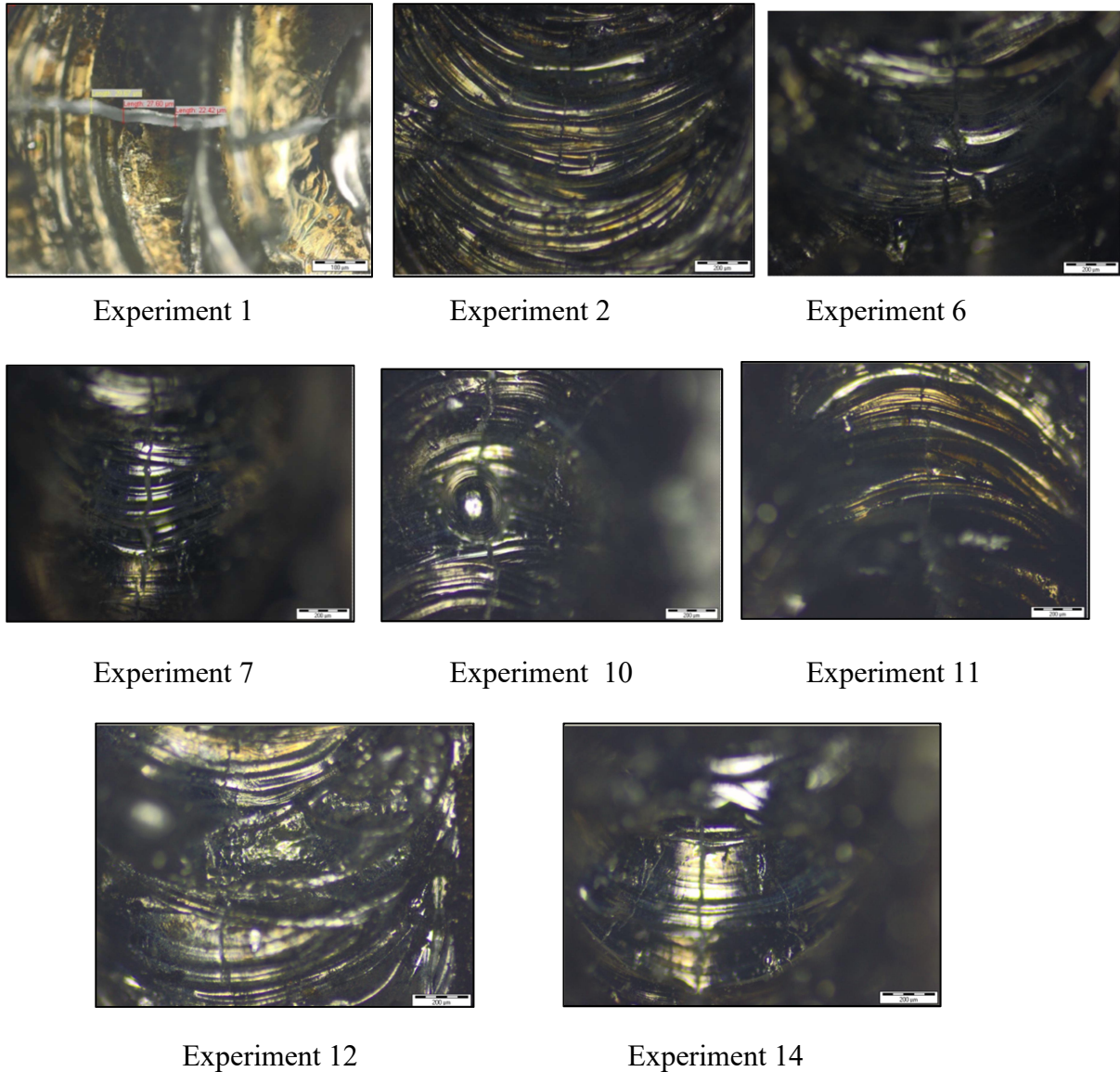


Fig. 3.48 Crack present in welded butt joint specimen

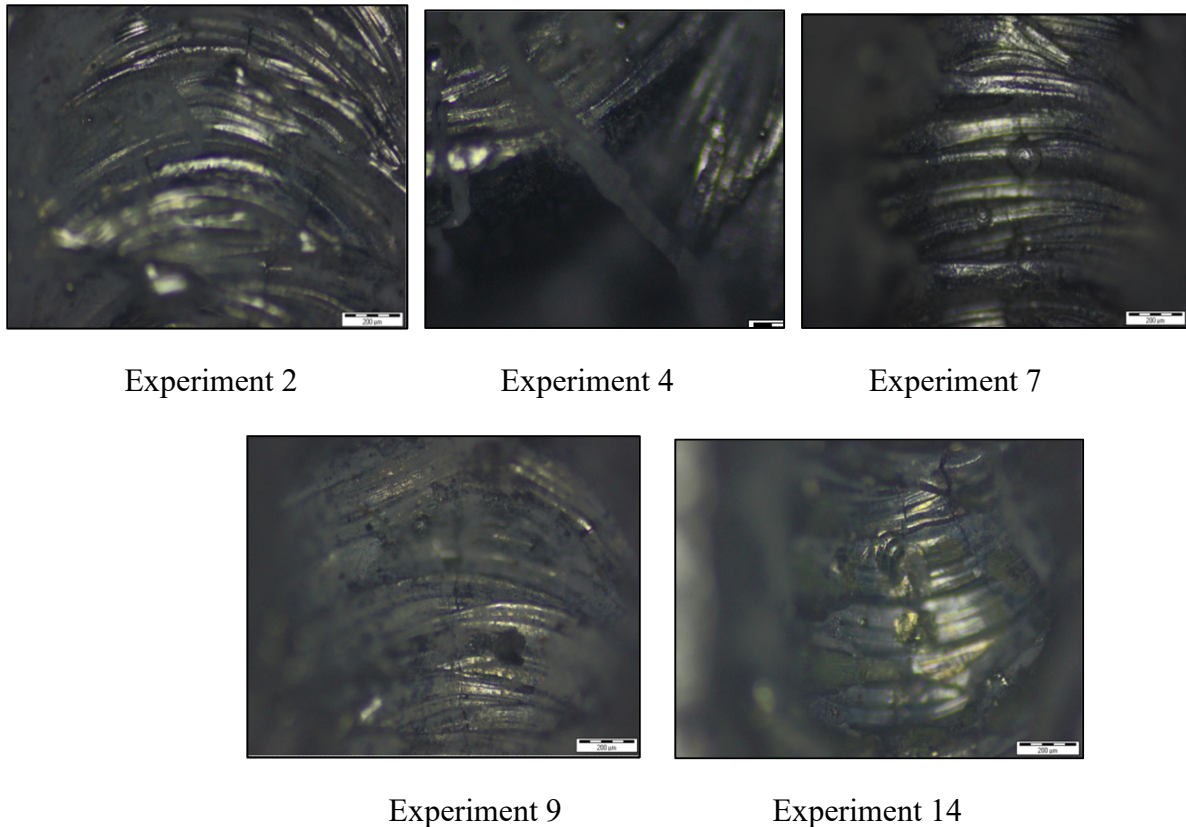


Fig. 3.49 Pores present in the laser welded butt joint specimen

It can be observed by examining cracks and pores present in the butt welded samples that at higher scanning speed larger number of cracks are seen and the intensity of cracks reduced with the scanning speed irrespective of peak power. As scanning speed is higher the time for energy transfer for a particular weld joint is reduced, the energy density is also reduced and instead of keyhole penetration, partial penetration occurred, that results different cracks in weld.

The pulse on time also played an important role for cracks and it is observed that the intensity of cracks is higher at low duty cycles.

The porosity is also prominently seen with cracks with lower intensity at lower peak powers. At lower peak power, keyhole penetration does not occur, so the gas present in the weld gets trapped inside completely forming pores.

CHAPTER 4

GENERAL CONCLUSION AND FUTURE SCOPE

4.1 GENERAL CONCLUSION

In the present work, laser welding of aluminium alloy 2024 of 2mm thickness is performed. The entire welding process is carried out on Pulsed ND-YAG 300W with argon as shielding gas. The study of mechanical characterization and microscopic study on laser welded Al 2024 for lap and butt joint configurations were carried out. Due its high reflectivity and conductivity aluminium is one of the material which is very difficult to weld. Aluminium also very much prone towards pores and solidification cracks, which makes the stability of the weld lesser. After trying with several no of experiments with variable process parameters optimized parameters range were found. Assist gas had a important role to reduce the welding defects in aluminium weld, after trying different gases with different pressure, the assist gas was finalised and optimize d pressure was selected. The following conclusions are drawn from the current work:

For Lap joint configuration:

1. The experimental design is prepared by considering four parameters: peak power, scanning speed, frequency and pulse on time. Taguchi L9 orthogonal array is adopted for design of experiments.
2. The maximum bond width of 954.76 μm is obtained at a peak power of 4.79 kW scanning speed 1.5mm/s and a frequency of 8Hz. Maximum theoretical throat length obtained is 983.34 μm which is also obtained at the parameters that gave maximum bond width.
3. The highest breaking load is attained at the following parameters: peak power 4.79Kw, scanning speed 1 mm/s and frequency 7 Hz.
4. The S/N ratio yielded the following parameters for maximized breaking load: peak power : 4.79Kw, frequency : 7Hz, and scanning speed 2 mm/s and at a pulse width of 7 ms.

For the butt joint configuration

1. The experimental design is prepared for four parameters: peak power, scanning speed, frequency and pulse on time. Taguchi L16 orthogonal array is adopted for design of experiments using butt joint.
2. The maximum weld width of 2043.33 μm is obtained at a peak power of 4.5 Kw, 1mm/s scanning speed and frequency of 8 Hz at a pulse on time of 8ms and the minimum weld width is at 4Kw, 1mm/s, 6Hz and 5ms.
3. The S/N ratio has indicated that for a peak power of 4.0 kW, scanning speed 1mm/s, frequency of 6 Hz and pulse width of 5ms the weld width is minimized.
4. The Pareto chart of standardized effects on weld width has indicated that pulse width is the most influential parameter of all the four parameters under consideration.
5. The weld with higher scanning speed has shown larger number of cracks and the intensity of cracks reduced with the scanning speed irrespective of peak power.
6. The pulse on time also played an important role for cracks and it is observed that the intensity of cracks is higher at low duty cycles.
7. The porosity is also prominently seen with cracks with lower intensity at lower peak powers.
8. The shielding gas pressure is varied at regular steps from 1 bar till 4 bar and it is observed that at 3 bar the weld is satisfactory.

4.2 FUTURE SCOPE

After the completion of the thesis there are many aspects to study further on welding of aluminium alloys. The future scope of this research includes:

1. To study the surface characteristics elaborately by Scanning Electron Microscope and analyse the effect of each parameters on different surface characteristics.
2. More study and experiment can be done to make the weld stronger which also has less defects.
3. To get more good weld experiment can be done with different gas mixture with different gas ratio and pressure
4. Laser welding of different alloys can be done to examine the effects with change of parameters for different series.

REFERENCES

1. Davis JR. Alloying: Understanding the Basics. ASM International. DOI:10.1361/autb2001p351.
2. Bastian. B. J, Annette O'Brien. Welding Handbook. Ninth edition, Volume 5, Materials and applications. PART 2; American welding society.
3. Huntington CA, Eagar TW. Laser Welding of Aluminum and Aluminum Alloys. *Welding Journal*. 1983;62(4): 105–107.
4. Leong KH, Sabo KR, Sanders PG, Spawr WJ. Laser Welding of Aluminum Alloys. *Proceedings of Photonics West '97*. International Society for Optics and Photonics; 1997. p. 37–44.
5. Leong KH, Sabo KR, Altshuller B, Wilkinson TL, Albright CE. Laser beam welding of 5182 aluminum alloy sheet. *Journal of Laser Applications*. 1999;11(3): 109–118.
6. Zhao H, White DR, DebRoy T. Current issues and problems in laser welding of automotive aluminium alloys. *International Materials Reviews*. 1999;44(6): 238–266.
7. Bardin F, McBride R, Moore A, Morgan S, Williams S, Jones JDC, et al. Real time temperature measurement for process monitoring of laser conduction welding. *Proceedings of the 23rd International Congress on Applications of Lasers and Electro-Optics*. San Francisco, CA: Laser Institute of America; 2004. p. 1–24.
8. Hu B, Richardson IM. Autogenous laser keyhole welding of aluminum alloy 2024. *Journal of Laser Applications*. 2005;17(2): 70–80.
9. Sanchez-amaya JM, Boukha Z, Amaya-vazques MR, Botana FJ. Weldability of Aluminum Alloys with High-Power Diode Laser. *Welding Research*. 2012;91: 155–161.
10. Kawahito Y, Matsumoto N, Abe Y, Katayama S. Laser absorption characteristics in high-power fibre laser welding of stainless steel. *Welding International*. 2013;27(2): 129–135.
11. Alfieri V, Cardaropoli F, Caiazzo F, Sergi V. Porosity evolution in aluminum alloy 2024 bop and butt defocused welding by Yb-YAG disk laser. *Engineering Review*. 2011;31(2): 125–132.

12. Caiazza F, Alfieri V, Cardaropoli F, Sergi V. Butt autogenous laser welding of AA 2024 aluminium alloy thin sheets with a Yb:YAG disk laser. *International Journal of Advanced Manufacturing Technology*. 2013;67: 2157–2169.
13. Enz J, Khomenko V, Riekehr S, Ventzke V, Huber N, Kashaev N. Single-sided laser beam welding of a dissimilar AA2024–AA7050 T-joint. *Materials & Design*. 2015;76: 110–116.
14. El-Batahgy A-M, Kutsuna M. Laser Beam Welding of AA5052, AA5083, and AA6061 Aluminum Alloys. *Research Letters in Materials Science*. 2009;2009: 1–9.
15. Okon P, Dearden G, Watkins K, Sharp M, French P. Laser welding of aluminium alloy 5083. *Proceedings of the 21st International Congress on Applications of Lasers and Electro-Optics*. Scottsdale, AZ: Laser Institute of America; 2002. p. 1–9. 268.
16. Weston JP, Jones IA, Wallach ER. Laser welding of aluminium alloys using different laser sources. *Proceedings of the 6th International Conference on Welding and Melting by Electron and Laser Beams*. Toulon: International Institute of Welding; 1998.
17. Sanchez-amaya JM, Boukha Z, Amaya-vazques MR, Botana FJ. Weldability of Aluminum Alloys with High-Power Diode Laser. *Welding Research*. 2012;91: 155–161.
18. Brown RT. Keyhole welding studies with a moderate-power, high-brightness fiber laser. *Journal of Laser Applications*. 2008;20(4): 201.
19. Squillace A, Prisco U. Influence of filler material on micro- and macro-mechanical behaviour of laser-beam-welded T-joint for aerospace applications. *Proceedings of the Institution of Mechanical Engineers, Part L: Journal of Materials: Design and Applications*. 2009;223(3): 103–115.
20. Shakeri HR, Buste a., Worswick MJ, Clarke J a., Feng F, Jain M, et al. Study of damage initiation and fracture in aluminum tailor welded blanks made via different welding techniques. *Journal of Light Metals*. 2002;2(2): 95–110.
21. Choi K-D, Ahn Y-N, Kim C. Weld strength improvement for Al alloy by using laser weaving method. *Journal of Laser Applications*. 2010;22(3): 116.
22. Fabrègue D, Deschamps A. Microstructural Study of Laser Welds Al6056-AS12 in Relation with Hot Tearing. *Materials Science Forum*. 2002;396-402: 1567–1572.

23. Li M, Li Z, Zhao Y, Li H, Wang Y, Huang J. Influence of Welding Parameters on Weld Formation and Microstructure of Dual-Laser Beams Welded T-Joint of Aluminum Alloy. *Advances in Materials Science and Engineering*. 2011;2011: 1–6.
24. Yang ZB, Tao W, Li LQ, Chen YB, Li FZ, Zhang YL. Double-sided laser beam welded T-joints for aluminum aircraft fuselage panels: Process, microstructure, and mechanical properties. *Materials & Design*. 2012;33: 652–658.
25. Liu C, Northwood D., Bhole S. Tensile fracture behavior in CO₂ laser beam welds of 7075-T6 aluminum alloy. *Materials & Design*. 2004;25(7): 573–577.
26. Weston JP, Jones IA, Wallach ER. Laser welding of aluminium alloys using different laser sources. *Proceedings of the 6th International Conference on Welding and Melting by Electron and Laser Beams*. Toulon: International Institute of Welding; 1998.
27. Squillace A, Prisco U. Influence of filler material on micro- and macro-mechanical behaviour of laser-beam-welded T-joint for aerospace applications. *Proceedings of the Institution of Mechanical Engineers, Part L: Journal of Materials: Design and Applications*. 2009;223(3): 103–115.
28. Caiazza F, Alfieri V, Cardaropoli F, Sergi V. Butt autogenous laser welding of AA 2024 aluminium alloy thin sheets with a Yb:YAG disk laser. *International Journal of Advanced Manufacturing Technology*. 2013;67: 2157–2169.
29. Cui L, Li X, He D, Chen L, Gong S. Effect of Nd:YAG laser welding on microstructure and hardness of an Al–Li based alloy. *Materials Characterization*. 2012;71: 95–102.
30. Wang J, Wang H-P, Wang X, Cui H, Lu F. Statistical analysis of process parameters to eliminate hot cracking of fiber laser welded aluminum alloy. *Optics & Laser Technology*. Elsevier, 2015;66: 15–21.
31. Wang X, Lu F, Wang H-P, Cui H, Tang X, Wu Y. Mechanical constraint intensity effects on solidification cracking during laser welding of aluminum alloys. *Journal of Materials Processing Technology*. 2015;218: 62–70.
32. Passini A, Oliveira AC De, Riva R, Travessa DN, Cardoso KR. Ultrasonic inspection of AA6013 laser welded joints. *Materials Research*. 2011;14(3): 417–422.
33. Lima MS, Riva R, Oliveira AC De, Siqueira GR. Laser beam welding aerospace aluminum using fiber lasers. In: Dreischuh T, Atanasov PA, Sabotinov N V. (eds.)

Proceedings of the 17th International Symposium on Gas Flow and Chemical Lasers and High Power Lasers. International Society for Optics and Photonics.; 2008. p. 713128. 270.

34. Katayama S, Nagayama H, Mizutani M, Kawahito Y. Fibre laser welding of aluminium alloy. *Welding International*. 2009;23(10): 744–752.

35. Oliveira AC, Siqueira RHM, Riva R, Lima MSF. One-sided laser beam welding of autogenous T-joints for 6013-T4 aluminium alloy. *Materials & Design*. 2015;65: 726–736.

36. de Siqueira RHM, de Oliveira AC, Riva R, Abdalla AJ, Baptista CARP, de Lima MSF. Mechanical and microstructural characterization of laser-welded joints of 6013-T4 aluminum alloy. *Journal of the Brazilian Society of Mechanical Sciences and Engineering*. 2015;37(1): 133–140.

37. Wang XJ, Lu FG, Wang HP, Cui HC, Tang XH, Wu YX. Experimental and numerical analysis of solidification cracking behaviour in fibre laser welding of 6013 aluminium alloy. *Science and Technology of Welding and Joining*. 2015;20(1): 58–67.

38. Gao M, Chen C, Hu M, Guo L, Wang Z, Zeng X. Characteristics of plasma plume in fiber laser welding of aluminum alloy. *Applied Surface Science*. 2015;326: 181–186.

39. Kawahito Y, Matsumoto N, Abe Y, Katayama S. Laser absorption of aluminium alloy in high brightness and high power fibre laser welding. *Welding International*. 2012;26(4): 275–281.

40. Kawahito Y, Matsumoto N, Abe Y, Katayama S. Laser absorption characteristics in high-power fibre laser welding of stainless steel. *Welding International*. 2013;27(2): 129–135.

41. Kawahito Y, Matsumoto N, Abe Y, Katayama S. Relationship of laser absorption to keyhole behavior in high power fiber laser welding of stainless steel and aluminum alloy. *Journal of Materials Processing Technology*. 2011;211(10): 1563–1568.

42. Yu Y, Wang C, Hu X, Wang J, Yu S. Porosity in fiber laser formation of 5A06 aluminum alloy. *Journal of Mechanical Science and Technology*. 2010;24(5): 1077–1082.

43. Paleocrassas AG, Tu JF. Low-speed laser welding of aluminum alloy 7075-T6 using a 300-W, single-mode, ytterbium fiber laser. *Welding Journal*. 2007;86: s179–s186.

44. Zhang ZH, Dong SY, Wang YJ, Xu BS, Fang JX, He P. Study on microstructures and mechanical properties of super narrow gap joints of thick and high strength aluminum alloy plates welded by fiber laser. *The International Journal of Advanced Manufacturing Technology*.2015; 271.
45. Zhang Z, Dong S, Wang Y, Xu B, Fang J, He P. Microstructure characteristics of thick aluminum alloy plate joints welded by fiber laser.*Materials & Design*. 2015;84: 173–177.
46. Allen CM, Verhaeghe G, Hilton PA, Heason CP, Prangnell PB. Laser and Hybrid Laser-MIG Welding of 6.35 and 12.7mm Thick Aluminium Aerospace Alloy. *Materials Science Forum*. 2006;519-521: 1139–1144.
47. Brown RT. Keyhole welding studies with a moderate-power, high-brightness fiber laser. *Journal of Laser Applications*. 2008;20(4): 201.
48. Shiganov IN, Kholopov AA, Ioda EI. Special features of laser welding of aluminium alloys.*Welding International*. 2012;26(3): 231–235.
49. Chu.Q, Bai.R., Jian.H., Lei.Z., Hu.N., & Yan.C. Microstructure, texture and mechanical properties of 6061 aluminum laser beam welded joints. *Materials Characterization*, 2018. 137, 269–276. doi:10.1016/j.matchar.2018.01.030.
50. Majumdar.J.D, Manna.I. *Laser-Assisted Fabrication of Materials*. Springer Series in Materials Science. 2013. DOI 10.1007/978-3-642-28359-8.